tentials, the reorganizational barriers for electron transfer to the metal center, and the extent of deprotonation of the ligand. The metal-centered oxidations of $Co^{II}(N_4)$, $Ni^{II}(N_4)$, and $Cu^{II}(N_4)$ all involve appreciable barriers; in each case the barrier to electron transfer seems to be largely Franck–Condon in origin.

Registry No. $Fe(phen)_3^{3+}$, 13479-49-7; $[Co(Me_2[14]4,7\text{-diene } N_4)Cl_2]ClO_4$, 83916-53-4; $[Co(Me_2[14]4,7\text{-diene } N_4)(OH_2)_2](PF_6)_2$, 83862-34-4; $[Co(Me_2[14]4,7\text{-diene } N_4)(NCS)_2]ClO_4$, 83916-54-5; $[Ni(Me_2[14]4,7\text{-diene } N_4)](ClO_4)_2$, 83916-55-6; $[Ni(Me_2[14]4,7\text{-dieno } N_4](ClO_4)_2$, 83862-36-6; $[Ni(Me_2[13]4,7\text{-diene } N_4](ClO_4)_2$, 83862-37-7; $[Ni(Me_2[13]4,7\text{-dieno } N_4]ClO_4$, 30649-42-4; $Co(Me_2[14]4,7\text{-dieno } N_4)(NCS)_2$, 73104-21-9; $Co(Me_2[14]4,7\text{-diene } N_4)(OH_2)_2^{3+}$, 61359-48-6; $[Ni(Me_2[14]4,7\text{-diene } N_4)](PF_6)_2$, 39561-16-5; $Cu(Me_2[14]4,7\text{-diene } N_4)^{2+}$, 46754-89-6; $Co(OH_2)_5Cl^{2+}$, 83862-38-8; $[Ni(Me_2[14]4,7\text{-dieno } N_4)]PF_6$, 39042-83-6; $[Cu(Me_2[14]4,7\text{-diene } N_4)](PF_6)_2$, 39561-21-2; $[Cu(Me_2[14]4,7\text{-dieno } N_4)]PF_6$, 39561-20-1.

Supplementary Material Available: Tables of elemental analyses and kinetic data; figures of pH titrations, cyclic voltammograms, and kinetic plots (16 pages). Ordering information is given on any current masthead page.

Kinetics, Thermodynamics, and Mechanism of the Radical Chain Process for Ligand Substitution of Metal Carbonyls

J. W. Hershberger, R. J. Klingler, and J. K. Kochi*

Contribution from the Department of Chemistry, Indiana University, Bloomington, Indiana 47405. *Received May 27, 1982*

Abstract: The radical chain process for the ligand substitution of a variety of carbonylmanganese derivatives ($\overline{Mn}L$) can be induced chemically or electrochemically with turnover numbers that can exceed 10^3. The catalytic cycle is initiated by electron transfer to afford the 17-electron carbonylmanganese cation $\overline{Mn}L^+$. The propagation steps in the chain process are (1) the facile ligand exchange of $\overline{Mn}L^+$ with the added nucleophile L to afford $\overline{Mn}L^+$ followed by (2) the reduction of $\overline{Mn}L^+$ by a homogeneous process involving cross electron exchange with $\overline{Mn}L$ and/or heterogeneous electron transfer at the electrode. This carbonylmetal system is sufficiently well behaved to allow the kinetics and thermodynamics for each step of the catalytic cycle to be examined in quantitative detail by transient and bulk electrochemical techniques. Analysis of the reversible cyclic voltammograms of $\overline{Mn}L$, both in the presence and in the absence of the nucleophile L, is achieved by Feldberg's digital simulation method. The computer simulation of the experimental cyclic voltammograms provides accurate values of the second-order rate constants for the rapid ligand exchange of $\overline{Mn}L^+$ with a variety of added nucleophiles L. The unusual reactivity patterns for substitution in the paramagnetic $\overline{Mn}L^+$ are presented in the context of previous studies with other metal carbonyls.

Ligand substitution of metal carbonyls plays a key role in the catalytic sequences of a variety of important processes leading to carbon monoxide fixation.[1,2] The conventional associative and dissociative mechanisms for such exchanges are usually considered to involve even-numbered, 16- and 18-electron intermediates.[3] Thus the recent reports of efficient chain mechanisms of ligand substitution in metal carbonyls involving odd-electron, radical intermediates merit special attention.[4,5]

Electrochemical techniques are well-suited for the study of radical chain mechanisms of ligand substitution, since the electron transfer to and from the diamagnetic metal carbonyls can be finely tuned to the electrode potential. Indeed we recently showed that electrocatalysis in the ligand substitution of a variety of otherwise stable group 6B metal carbonyls such as $(py)W(CO)_5$ is initiated by anodic oxidation to the 17-electron radical cation (i.e., $(py)W(CO)_5^+$), which is the species labile to substitution.[6] In order to probe the mechanistic details of this novel type of chain substitution, it is desirable to choose a metal carbonyl system of high catalytic efficiency and one in which the electrode process is well-behaved. Accordingly, we have focussed our attention in this paper on the carbonylmanganese derivatives η^5-$MeCpMn(CO)_2L$,[7] hereafter referred to as $\overline{Mn}L$. The choice of this metal carbonyl was dictated by the high current efficiencies attainable for ligand substitution by various nucleophiles L at the electrode [E], i.e.:

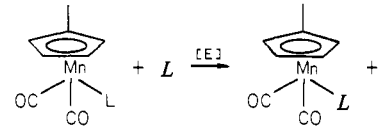

(1)

Importantly, the oxidation–reduction of both $\overline{Mn}L$ and $\overline{Mn}L$ are electrochemically reversible on the cyclic voltammetric time scale.

Previous studies of ligand substitution in these manganese carbonyls have been mostly photochemical,[8,9] since the replacement

(1) Wender, I., Pino, P., Eds. "Organic Synthesis via Metal Carbonyls"; Wiley-Interscience: New York, (a) 1968; Vol. 1; (b) 1976; Vol. 2.
(2) (a) Pruett, R. L. *Adv. Organomet. Chem.* **1979**, *17*, 1. Forster, D. *Ibid.* *17*, 255. Masters, C. *Ibid.* C1. (b) Heck, R. F. "Organotransition Metal Chemistry"; Academic Press: New York, 1974.
(3) (a) Basolo, F., Pearson, R. G. "Mechanisms of Inorganic Reactions", 2nd ed.; Wiley-Interscience: New York, 1967; p 533. (b) Dobson, G. R. *Acc. Chem. Res.* **1976**, *9*, 300. (c) Deeming, A. J. *Inorg. React. Mech.* **1981**, *7*, 275 and related reviews in this series.
(4) (a) Kidd, D. R.; Brown, T. L. *J. Am. Chem. Soc.* **1978**, *100*, 4095. (b) Byers, B. H.; Brown, T. L. *Ibid.* **1975**, *97*, 947. (c) *Ibid.* **1977**, *99*, 2527. (d) Byers, B. H.; Brown, T. L. *J. Organomet. Chem.* **1977**, *127*, 181. (e) Hoffman, H. W.; Brown, T. L. *Inorg. Chem.* **1978**, *17*, 613. (f) Absi-Halabi, M.; Brown, T. L. *J. Am. Chem. Soc.* **1977**, *99*, 2982. (g) Absi-Halabi, M.; Atwood, J. D.; Forbus, N. P.; Brown, T. L. *Ibid.* **1980**, *102*, 6248.
(5) (a) Bezems, G. J.; Rieger, P. H.; Visco, S. *J. Chem. Soc., Chem. Commun.* **1981**, 265. (b) Summers, D. P.; Luong, J. C.; Wrighton, M. S. *J. Am. Chem. Soc.* **1981**, *103*, 5238.
(6) Hershberger, J. W.; Klingler, R. J.; Kochi, J. K. *J. Am. Chem. Soc.* **1982**, *104*, 3034.
(7) For a preliminary report, see: Hershberger, J. W.; Kochi, J. K. *J. Chem. Soc., Chem. Commun.* **1982**, 212.
(8) (a) Strohmeier, W.; von Hobe, D. *Z. Phys. Chem. (Wiesbaden)* **1962**, *34*, 393. (b) Strohmeier, W.; Barbeau, C.; von Hobe, D. *Chem. Ber.* **1963**, *96*, 3254.

0002-7863/83/1505-0061$01.50/0

Table I. Electrocatalysis of the Ligand Exchange of Various Carbonylmanganese Derivatives $\overline{Mn}L$ by Added Nucleophiles L[a]

entry	$\overline{Mn}L$ (mmol)	L (mmol)	solvent	current, μA	m/n[b]
1	MeCN (0.48)	PPh_3 (0.48)	MeCN	100	1013
2	MeCN (0.48)	$CNCMe_3$ (0.48)	MeCN	100	365
3	MeCN (0.31)	$P(Me)Ph_2$ (0.40)	MeCN	50	1004
4	MeCN (0.19)	$P(C_6H_4Me\text{-}p)_3$ (0.20)	MeCN	50	748
5	MeCN (0.16)	$P(C_6H_4Cl\text{-}p)_3$[c] (0.20)	MeCN	50	139
6	MeCN (0.12)	$P(OMe)Ph_2$ (0.14)	MeCN	100	833
7	MeCN (0.13)	$P(OPh)_3$ (0.15)	MeCN	100	29
8	MeCN (0.12)	$P(OPh)_3$ (1.9)	MeCN	100	142
9	MeCN (0.11)	$P(OMe)_3$ (0.13)	MeCN	100	196
10	MeCN (0.19)	$AsPh_3$ (0.21)	MeCN	100	82
11	MeCN (0.17)	$SbPh_3$ (0.20)	MeCN	200	96
12	NC_5H_5 (py) (0.076)	PPh_3 (1.5)	Me_2CO	50	92
13	NC_5H_5 (py) (0.11)	PPh_3 (0.16)	Me_2CO	500	23
14	NC_5H_5 (py) (0.48)	PPh_3 (0.48)	MeCN	100	291
15	NC_5H_5 (py) (0.12)	$CNCMe_3$ (0.15)	Me_2CO	100	64
16	NC_5H_5 (py) (0.10)	PEt_3 (0.12)	Me_2CO	100	174
17	NC_5H_5 (py) (0.10)	$P(OPh)_3$ (1.9)	Me_2CO	1000	5.2
18	NC_5H_5 (py) (0.10)	$P(OPh)_3$ (2.0)	MeCN	500	95
19	$HN(CH_2)_5$ (0.10)	PEt_3 (0.53)	Me_2CO	4000	1.8[d]
20	$HN(CH_2)_5$ (0.16)	PEt_3 (4.0)	Me_2CO	4000	1.3[d]
21	THF (0.23)	PPh_3 (0.23)	THF[e]	500	56
22	THF (0.23)	MeCN (0.40)	THF[e]	1000	18
23	THF (0.23)	NC_5H_5 (py) (0.30)	THF[e]	1000	91
24	Me_2SO (0.12)	PPh_3 (0.14)	Me_2CO	100	33
25	Me_2SO (0.17)	PPh_3 (0.19)	MeCN	100	338
26	norbornene (0.18)	PPh_3 (0.19)	Me_2CO	1000	7.0[f]
27	norbornene (0.094)	PPh_3 (0.095)	MeCN	1000	71

[a] Controlled-current oxidations at a Pt-gauze electrode performed at 22 °C in 12 mL of solvent and afforded quantitative yields of product, unless otherwise noted. In acetone and MeCN, the supporting electrolyte was 0.1 N tetraethylammonium perchlorate (TEAP) and in THF, 0.1 N tetrabutylammonium perchlorate (TBAP) was employed. [b] Current efficiency, m/n, defined as the moles of starting material consumed divided by the faradays of charge passed through the solution. All current efficiencies are reported for the conversion of all the starting material. [c] The phosphine was incompletely dissolved at the outset of the electrolysis. [d] Product yield 80% by IR spectrophotometry. [e] Performed at 0 °C. [f] Product yield 85% by IR spectrophotometry.

of carbon monoxide in $CpMn(CO)_3$ and of various ligands L in $CpMn(CO)_2L$ occurs readily upon actinic irradiation.[10] By contrast, the thermal activation of ligand substitution has received less attention owing to slow rates of substitution. For example, temperatures in excess of 200 °C are said to be required to replace CO in $CpMn(CO)_3$ with a phosphine or arsine ligand.[11]

Results

We have observed similar inactivity in the ordinary thermal substitution of the ligand L from $MeCpMn(CO)_2L$. Thus the replacement of pyridine by the phosphine in eq 2 proceeds only

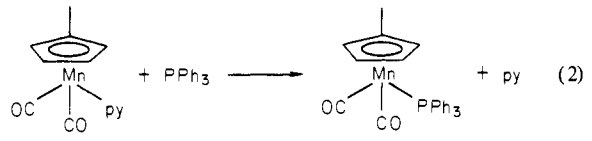

(2)

upon refluxing a toluene solution overnight. At a lower temperature (65 °C), $\overline{Mn}$(py) was recovered quantitatively after 4 h. By contrast, the stimulus provided by an electrical current leads to an efficient ligand substitution at much lower temperatures, as described below.

I. Electrocatalysis of Ligand Substitution in Manganese Carbonyls. The phosphine substitution of $\overline{Mn}$(NCMe) in eq 2 is complete at 22 °C within 12 min if a mere trickle of electrical current is passed through the acetonitrile solution (containing 0.1 M tetraethylammonium perchlorate (TEAP) as supporting electrolyte) with the aid of a set of platinum electrodes. *Electrocatalysis* is readily deduced by coulometry during the bulk electrolysis carried out at either constant potential or at constant current.[12] From the measurement of the amount of charge (faradays) passed through the solution, a current efficiency in excess of 290 equiv of $\overline{Mn}$(py) was obtained per electron. A catalytic cycle with a long kinetic chain length is thus indicated for this electrochemical process.

The rate of ligand substitution under electrostimulation is visually apparent by the gradual color change from orange of $\overline{Mn}$(py) to the faint yellow color of the product. It could be followed quantitatively by monitoring the carbonyl bands by infrared spectrophotometry of both the reactant [ν(CO) of $\overline{Mn}$(py), 1934, 1868 cm^{-1}] and the product [ν(CO) of $\overline{Mn}(PPh_3)$, 1884, 1944 cm^{-1}]. The final yield of $\overline{Mn}(PPh_3)$ was 96%, determined spectrophotometrically (±7%). The product was isolated in 64% yield by precipitation and compared with an authentic sample of $MeCpMn(CO)_2PPh_3$ prepared independently (see Experimental Section).

The course of ligand substitution can also be followed electrochemically by periodically monitoring the electrode potential during a run carried out at constant current. For example, the starting potential of −0.13 V vs. saturated NaCl SCE at the platinum gauze anode shown in Figure 1 reflects the oxidation of $\overline{Mn}$(py). The consumption of $\overline{Mn}$(py) is accompanied by a gradual increase in the electrode potential until that time (t = 12 min) at which there is a sharp rise in potential owing to the complete disappearance of $\overline{Mn}$(py). The attainment of the new plateau at 0.28 V heralds the anodic oxidation of the product, which can be confirmed by examining the electrode potential of a fresh solution of $\overline{Mn}(PPh_3)$ under equivalent conditions.

II. Structural Effects and the Efficiency of Electrocatalytic Substitution. The electrocatalytic procedure for substitution allows

(9) Giordano, P. J.; Wrighton, M. W. *Inorg. Chem.* **1977**, *16*, 160.
(10) (a) Strohmeier, W.; Barbeau, C. *Z. Naturforsch., B: Anorg. Chem., Org. Chem., Biochem., Biophys. Biol.* **1962**, *17B*, 848. (b) King, R. B.; Zipperer, W. C.; Ishaq, M. *Inorg. Chem.* **1972**, *11*, 1361. (c) Nyholm, R. S.; Sandhu, S. S.; Stiddard, M. H. B. *J. Chem. Soc.* **1963**, 5917. (d) Connelly, N. G.; Kitchen, M. D. *J. Chem. Soc., Dalton Trans.* **1977**, 931.
(11) See ref 1a, p 139, and ref 10c.
(12) We generally found the electrocatalysis at constant current to be preferable to that at constant potential, since it allowed the oxidized species to be generated at less than diffusion-limited rates. The resulting catalytic processes were highly efficient and less subject to the destruction of $\overline{Mn}L$.

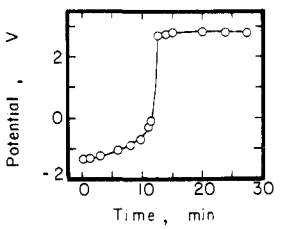

Figure 1. Variation in the electrode potential during the electrocatalytic substitution of 4.0×10^{-2} M $MeCpMn(CO)_2py$ with 4.0×10^{-2} M PPh_3 in 12 mL of MeCN solution containing 0.1 M TEAP at a controlled current of 100 μA at 22 °C.

a variety of ligands ***L*** to be readily incorporated into the carbonylmanganese moiety. For example, starting with either the

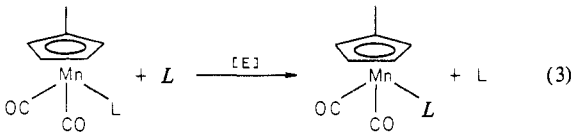

acetonitrile or the pyridine complex $\overline{Mn}(NCCH_3)$ or $\overline{Mn}(py)$, the various alkyl and arylphosphines and phosphites ***L*** listed in Table I partake in electrocatalytic substitutions with high current efficiencies. In accord with the latter, the yields of the phosphine substitution products were essentially quantitative to within the precision of infrared spectrophotometry (see Experimental Section). Arsines and stibines as well as alkyl isocyanides are also efficiently incorporated.

For each pair of reactants in Table I, the appropriate control experiment was performed in the absence of an anodic current to ensure that the background, thermal reaction was unimportant. Indeed the solutions were initially prereduced under a nitrogen or argon atmosphere at a negative potential—typically −0.5 V, at which none of the components is electroactive—to preclude adventitious (oxidized) impurities from catalyzing the thermal process.[13] Under these conditions, none of the substitutions were found to proceed at room temperature in the absence of electrostimulation, certainly for at least twice the duration of the electrocatalytic experiment or 1 h, whichever was longer.[15,16] The exception was the tetrahydrofuran (THF) derivative $\overline{Mn}(THF)$, which, by itself, is highly labile even at 0 °C and slowly undergoes spontaneous substitution with added ligands such as PPh_3, py, and MeCN.[17] However, the extent of this thermal process is minor in eq 4 (~20% conversion after 1 h), compared to the electro-

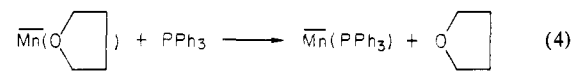

catalytic substitution carried out at 0.5 mA, which leads to 100% conversion after 13 min, as listed in entry 21, Table II.

The effectiveness of electrocatalytic substitution can be judged in two ways. First, the last column in Table I lists the current efficiency as measured by the reciprocal of the total charge n (faraday) passed through the solution per mole m of starting material. As such, it represents a minimum value of the catalytic efficiency, or equivalently, the kinetic chain length of the radical process. The efficiency is dependent on both the nature of the displaced and substituting ligands L and ***L***, as well as the bulk concentration of ***L***. For example, the current efficiency for the replacement of acetonitrile in $\overline{Mn}(NCMe)$ is 3 times greater than pyridine substitution in $\overline{Mn}(py)$ and dimethyl sulfoxide substitution in $\overline{Mn}(Me_2SO)$, and more than 150 times greater than norbornylene substitution in $\overline{Mn}(NB)$ when PPh_3 is used as the common nucleophile under standard reaction conditions. Electrocatalytic substitution by added phosphines is more effective than that by phosphites. Thus the current efficiency for the electrocatalysis of $\overline{Mn}(NCMe)$ by the added nucleophiles PPh_3 and $P(OMe)Ph_2$ is exceedingly high ($>10^3$), despite their presence in only equimolar amounts. Under equivalent conditions, the current efficiency for the utilization of the weaker $P(OPh)_3$ is only ~30. Moreover when the concentration of $P(OPh)_3$ is increased 10-fold, the current efficiency rises to >140.

Acetonitrile is a considerably more effective solvent than acetone for electrocatalytic substitution in this series of manganese carbonyls. Thus the current efficiencies in acetonitrile are higher by a factor of more than 10 relative to those carried out in acetone (compare the pairs of entries 13–14, 17–18, and 24–25 in Table I). Furthermore, acetonitrile is an effective solvent for substitution even when it is present as a ligand to be displaced in the complex $\overline{Mn}(NCMe)$. Likewise, tetrahydrofuran can be used as the solvent for the substitution of $\overline{Mn}(THF)$ with triphenylphosphine, pyridine, and acetonitrile.

III. Transient Electrochemical Behavior of Manganese Carbonyls at the Anode, with and without Added Nucleophiles. In order to probe the origin of the electrocatalysis in ligand substitution, we examined the transient electrochemical behavior of the manganese carbonyls in Table I, both in the absence and presence of

Table II. Reversible CV Parameters of Various Carbonylmanganese Derivatives $\overline{Mn}L$[a]

entry	L	solvent	E_p^{ox}, V	$(E_p^{ox} + E_p^{red})/2$, V	i_p^a/i_p^c
1	$HN(CH_2)_5$	Me_2CO	0.02	−0.04	1.1
2	NC_5H_5(py)	Me_2CO	0.14	0.11	1.0
3	MeCN	Me_2CO[b]	0.18	0.12	1.0
4	MeCN	CH_2Cl_2[c]	0.20	0.15	1.0
5	MeCN	MeCN	0.22	0.19	1.0
6	PEt_3	Me_2CO	0.44	0.40	1.0
7	norbornene	MeCN[d]	0.49	0.44	1.1
8	$P(Me)Ph_2$	MeCN	0.53	0.49	1.0
9	$P(C_6H_4Me\text{-}p)_3$	MeCN	0.53	0.50	1.0
10	PPh_3	MeCN	0.55	0.52	1.0
11	PPh_3	Me_2CO	0.55	0.52	1.0
12	$CNCMe_3$	MeCN	0.58	0.53	1.0
13	$CNCMe_3$	Me_2CO	0.59	0.54	1.0
14	$P(C_6H_4Cl\text{-}p)_3$	MeCN	0.64	0.60	1.0
15	$P(OMe)Ph_2$	MeCN	0.65	0.62	1.0
16	$P(OMe)_3$	MeCN	0.72	0.68	1.0
17	$P(OPh)_3$	MeCN	0.91	0.85	1.0
18	CO	MeCN[e]	1.20	1.15	1.0
19	THF	THF[f]	0.09		
20	$AsPh_3$	MeCN	0.55		
21	$SbPh_3$	MeCN	0.65		
22	Me_2SO	MeCN	0.73		
23	SO_2	Me_2CO	1.06[g]		

[a] Cyclic voltammetry performed at a Pt microelectrode with solutions 10^{-3} M in substrate and 0.1 N in supporting electrolyte (tetraethylammonium perchlorate for MeCN or acetone, tetrabutylammonium perchlorate for THF or CH_2Cl_2). Unless otherwise noted, the scan rate was 100 mV s^{-1} and $T = 22$ °C. Potentials reported relative to the Cp_2Fe/Cp_2Fe^+ couple taken to have $(E_p^{ox} + E_p^{red})/2 = 0.31$ V in all solvents. [b] Scan rate = 50 mV s^{-1}, $T = -55$ °C. [c] Scan rate = 800 mV s^{-1}. [d] Scan rate = 200 mV s^{-1}, $T = -50$ °C. [e] Scan rate = 200 mV s^{-1}, $T = -28$ °C. [f] Scan rate = 30 mV s^{-1}. [g] Value difficult to reproduce owing to the rapid deactivation of the Pt electrode.

(13) Since a prolonged exposure to roomlight may induce the ligand exchange,[9,14] the electrocatalysis was performed in either subdued light or in a foil-covered apparatus.

(14) Roomlight produces ligand exchange pseudoequilibria in substituted group 6 carbonyls. See: Nasielski, J.; Vermeulen, M.; Leepoel, P. *J. Organomet. Chem.* **1975**, *102*, 195.

(15) In practice, the anodic current was selected to afford a convenient reaction time, usually between 10 and 60 min. Current efficiencies were found to be more or less independent of the current.

(16) These reactions were difficult to monitor by IR spectrophotometry in some cases (such as the exchange between $\overline{Mn}(NCMe)$ and PPh_2Me or $P(OMe)_3$), which appeared to be induced by the NaCl windows of the solution cells.

(17) The rapid substitution of $\overline{Mn}(THF)$ is described in the Experimental Section. It was thus not used in pure form but stored in solution at −78 °C.

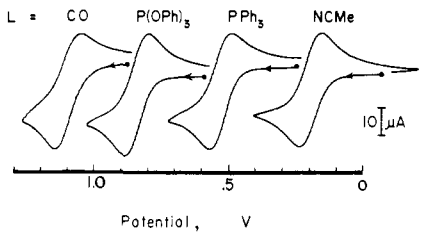

Figure 2. Systematic variation in $E°$ for various carbonylmanganese derivatives $\overline{\text{Mn}}\text{L}$, as shown by the reversible cyclic voltammograms recorded at a sweep rate of 100 mV s^{-1} in acetonitrile containing at 0.1 M TEAP at 22 °C (except for $\overline{\text{Mn}}(\text{CO})$ at −28 °C and 200 mV s^{-1}). L from left to right: CO, $P(OPh)_3$, PPh_3, NCMe.

added nucleophiles ***L***. The cyclic voltammetry (CV) was carried out at a stationary platinum microelectrode in acetonitrile, methylene chloride, or acetone solutions containing 0.1 M tetraalkylammonium perchlorates as supporting electrolytes.

A. Cyclic Voltammograms (CV) of $\overline{\text{Mn}}\text{L}$. The initial anodic scans for the cyclic voltammograms of the pyridine, triphenylphosphine, and carbon monoxide derivatives of $MeCpMn(CO)_2L$ in Figure 2 are all characterized by ratios of the anodic and cathodic currents (i_p^a/i_p^c) of unity and by anodic and cathodic peak separations ($E_p^a - E_p^c$) of near 60 mV for reversible one-electron processes:

$$MeCpMn(CO)_2L \overset{E°}{\rightleftharpoons} MeCpMn(CO)_2L^+ + e \qquad (5)$$

The magnitude of the reversible oxidation potentials $E°$ of the series of $\overline{\text{Mn}}\text{L}$ listed in Table II is strongly dependent upon the nature of the coordinated ligand L. Thus the nitrogen-centered ligands such as amines and nitriles effect the most negative values in the range $-0.04\text{ V} < E° < 0.19\text{ V}$. The reversible potentials of alkyl- and arylphosphine complexes are clustered around 0.5 ± 0.1 V, but those of corresponding phosphites are significantly more positive. Among carbon-centered ligands, the values of $E°$ become progressively more positive in the order: alkene (norbornene, 0.44 V) < isocyanide (*t*-BuNC, 0.53 V) << carbon monoxide (1.15 V).[18] Indeed, the potential of the carbon monoxide complex $MeCpMn(CO)_3$ is the most positive of the derivatives listed in Table II. We can deduce from these trends that the ease with which various $\overline{\text{Mn}}\text{L}$ are oxidized is qualitatively dependent on the σ-donor property of L and by its π acidity. For example, among complexes with nitrogen ligands, $E°$ becomes progressively more negative with increasing base strengths of L in the order: acetonitrile < pyridine << piperidine.[19] Moreover, we infer from the significantly more negative value of $E°$ for $\overline{\text{Mn}}(\text{CNBu-}t)$ compared to the $E°$ for $\overline{\text{Mn}}(\text{CO})$, that the ligand π acidities are in the order:[20] carbon monoxide > *tert*-butylisocyanide.[21]

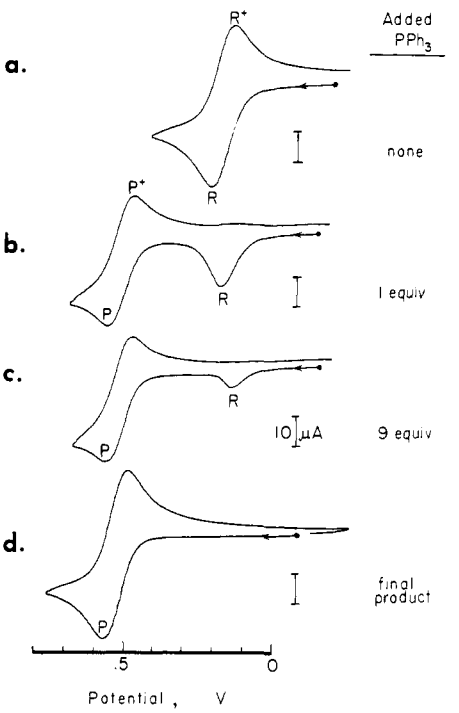

Figure 3. Dramatic effect of added PPh_3 on the reversible CV of 1.0×10^{-3} M $\overline{\text{Mn}}(\text{NCMe})$ in acetonitrile containing 0.1 M TEAP at a scan rate of 200 mV s^{-1} at 22 °C. The CV waves of $\overline{\text{Mn}}(\text{NCMe})$ R and $\overline{\text{Mn}}(PPh_3)$ P are indicated for solutions containing (a) 0, (b) 1, and (c) 9 equiv of added PPh_3. (d) CV of authentic $\overline{\text{Mn}}(PPh_3)$ under the same conditions.

B. Effect of Nucleophiles on the CV of $\overline{\text{Mn}}\text{L}$. The cyclic voltammetry of $\overline{\text{Mn}}\text{L}$ in the presence of added nucleophile ***L*** provides unique insight into the mechanism of electrocatalysis. Thus Figure 3 illustrates how the presence of triphenylphosphine leads to a drastic alteration of the well-behaved, reversible CV of $\overline{\text{Mn}}(\text{NCMe})$. In particular, the reactant wave [R = $\overline{\text{Mn}}$(NCMe)] in Figure 3b becomes clearly irreversible, as indicated by the absence of the coupled cathodic wave shown in Figure 3a. Furthermore, the anodic peak current i_p^a for $\overline{\text{Mn}}(\text{NCMe})$ decreases in magnitude in proportion to the concentration of PPh_3 (compare Figure 3 b and c), and the diffusion current falls to near zero. This behavior requires that $\overline{\text{Mn}}(\text{NCMe})$ be removed from the vicinity of the electrode by some alternative process that does not require a net flow of current. Such a process simultaneously leads to the substitution product [P = $\overline{\text{Mn}}(PPh_3)$], which is clearly in evidence in Figure 3 b and c, by its reversible CV wave at the higher potential of $E° = 0.55$ V. In other words, the anodic electrode process leading to the depletion of $\overline{\text{Mn}}(\text{NCMe})$ also results in the concomitant formation of $\overline{\text{Mn}}(PPh_3)$. Since the electrode process at $E = 0.22$ V is one in which the 17-electron cation $\overline{\text{Mn}}(\text{NCMe})^+$ is generated, it must be the species involved in the ligand exchange to afford the substitution product:

$$\overline{\text{Mn}}(\text{NCMe})^+ + PPh_3 \rightarrow \overline{\text{Mn}}(PPh_3)^+ + \text{MeCN} \qquad (6)$$

Indeed the experiments to be described in the following section will show that the cation is significantly more reactive to phosphine substitution than its neutral, diamagnetic precursor $\overline{\text{Mn}}(\text{NCMe})$.

C. Substitution Lability of Cationic Manganese Carbonyls. Independent studies of the facile substitution of cations were carried out by the prior generation of $\overline{\text{Mn}}(\text{NCMe})^+$ as a deep orange solution. The bulk electrolysis of $\overline{\text{Mn}}(\text{NCMe})$ in aceto-

(18) The CVs of $\overline{\text{Mn}}(\text{CO})$ and $\overline{\text{Mn}}$(norbornene) are irreversible at scan rates of 100 mV s^{-1} and 25 °C but become quasi-reversible at lower temperatures and increasing scan rates.

(19) Ligand effects on the electrochemistry and photoelectron spectroscopy of metal carbonyls has recently been discussed. See: Bursten, B. E. *J. Am. Chem. Soc.* **1982**, *104*, 1299.

(20) For ambiguities in the separate evaluation of σ- and π-bonding effects, see: (a) Hubbard, J. L.; Lichtenberger, D. L. *J. Am. Chem. Soc.* **1982**, *104*, 2132. (b) Hall, M. B.; Sherwood, D. E. *Inorg. Chem.* **1980**, *19*, 1805.

(21) Connelly and co-workers[10d] have reported the electrochemical behavior of $(\eta^5\text{-}MeC_5H_4)Mn(CO)_{3-x}L_x$, where $x = 1, 2$ with L = PR_3 and $P(OR)_3$. They noted a linear correlation between E_p^{ox} and k(CO), the Cotton–Kraihanzel force constant.[22,23] However, when disparate ligands (such as those given in Table II) are included, we find that their relationship breaks down. [In the plot, we employed $(E_p^{ox} + E_p^{red})/2$ in Table II (as opposed to E_p^{ox}) when referring to a thermodynamic redox property of the carbonylmetal since the electrode kinetics could affect the location of the current maximum in a quasi-reversible system.[24]] Nonetheless, the qualitative trend for $E°$ to be more positive with ligands of higher π acidity is apparent.[25]

(22) Cotton, F. A.; Kraihanzel, C. S. *J. Am. Chem. Soc.* **1962**, *84*, 4432.

(23) (a) Connelly and co-worker have also reported correlations between E_p^{ox} and ν(CO). (b) Connelly, N. G.; Demidowicz, Z.; Kelly, R. L. *J. Chem. Soc., Dalton Trans.* **1975**, 2335. (c) Connelly, N. G.; Kelly, R. L. *J. Organomet. Chem.* **1976**, *120*, C16.

(24) Nicholson, R. S. *Anal. Chem.* **1965**, *37*, 1351.

(25) For a discussion of π acidity and the effect on ν(CO), see: Cotton, F. A.; Wilkinson, G. "Advanced Inorganic Chemistry", 4th ed.; Wiley-Interscience: New York, 1980; p 1070.

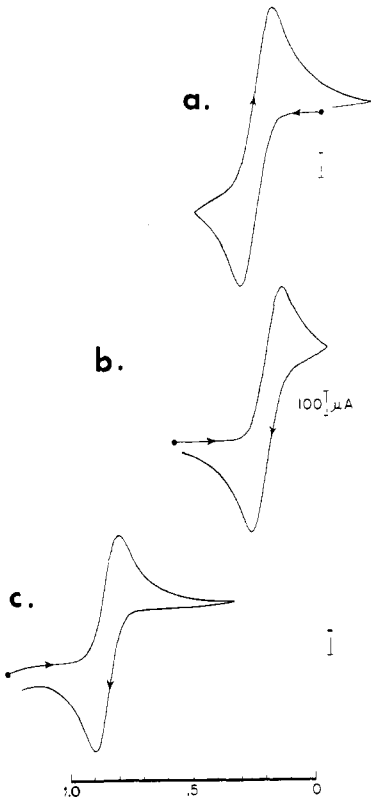

Figure 4. (a) Reversible oxidation of $\overline{Mn}(NCMe)$ in acetonitrile containing 0.1 M TEAP at −35 °C and a scan rate of 50 mV s^{-1}. (b) Reversible reduction of the solution in (a) after exhaustive oxidation at 0.5 V and −35 °C. (c) Cyclic voltammogram (initial negative scan) of the solution in (b) immediately after the addition of excess $P(OPh)_3$.

nitrile at a constant potential of +0.5 V required the passage of 1.0 faraday of charge per mole of $\overline{Mn}(NCMe)$: i.e.,

$$\overline{Mn}(NCMe) \xrightarrow{[E]} \overline{Mn}(NCMe)^+ + e \qquad (7)$$

Provided the temperature was not allowed to rise above −40 °C, the rereduction of $\overline{Mn}(NCMe)^+$ could be effected quantitatively back to the neutral precursor, as shown by the cyclic voltammogram in Figure 4b.

Addition of triphenyl phosphite to the solution of $\overline{Mn}(NCMe)^+$ at −40 °C immediately led to a deep orange-brown solution, which proved to contain only $\overline{Mn}[P(OPh)_3]^+$:

$$\overline{Mn}(NCMe)^+ + P(OPh)_3 \xrightarrow[-40\ °C]{fast} \overline{Mn}P(OPh)_3{}^+ + MeCN \qquad (8)$$

as shown by the cyclic voltammogram in Figure 4c. The same cationic product could be independently generated by the bulk electrolysis of $\overline{Mn}[P(OPh)_3]$ at +1.0 V.[26]

Similar results of facile cation substitution were obtained between triphenylphosphine and the pyridine analogue $\overline{Mn}(py)^+$, which was generated by the bulk electrolysis of $\overline{Mn}(py)$ in acetone at −30 °C:

$$\overline{Mn}(py)^+ + PPh_3 \rightarrow \overline{Mn}(PPh_3)^+ + py \qquad (9)$$

Bulk electrolysis of $\overline{Mn}(NCMe)$ and $\overline{Mn}(py)$ must be carried out at relatively low temperatures to minimize the decomposition of the labile cations $\overline{Mn}(NCMe)^+$ and $\overline{Mn}(py)^+$, respectively.[27]

(26) Note that $E°$ for $\overline{Mn}[P(OPh)_3]$ is sufficiently positive that there are complications in the cyclic voltammograms arising from the oxidation of the ligand. Such systems exhibit electrocatalytic oxidation of added phosphine nucleophiles (see: Hershberger, J. W.; Amatore, C.; Kochi, J. K. *J. Organomet. Chem.*, submitted for publication).

Consequently, it was not experimentally feasible to measure the rates of the cationic ligand substitutions described in eq 8 and 9 at the ambient temperatures employed in the electrocatalytic studies. Nonetheless, the facility with which such cationic substitutions occurs at temperatures below −30 °C does provide unequivocal grounds for their participation in the electrocatalytic cycles.

Electrocatalysis as described above implies the passage of current, however small, through the solution during ligand substitution. In the next section, we describe an alternative manifestation of the catalytic process.

IV. Chain Process for Ligand Substitution in the Absence of Current. If the passage of an electrical current through a solution of $\overline{Mn}(NCMe)$ and PPh_3 is abruptly interrupted, the ligand substitution continues on for a substantial period of time. The latter indicates that the substitution reaction in eq 10 can proceed

$$\overline{Mn}(NCMe) + PPh_3 \rightarrow \overline{Mn}(PPh_3) + MeCN \qquad (10)$$

at an appreciable rate even without a continual application of an electrode potential to the solution. To test this notion, we initially oxidized a very small portion (~2%) of $\overline{Mn}(NCMe)$ to the cation $\overline{Mn}(NCMe)^+$ at 0 °C, and then disconnected the electrochemical circuit. Upon the addition of PPh_3, the visual change of the solution containing $\overline{Mn}(NCMe)$ to the color $\overline{Mn}(PPh_3)$ was apparent within 30 s. Moreover, the substitution product could be

$$\overline{Mn}(NCMe) + PPh_3 \xrightarrow{[2\%\ Mn(NCMe)^+]} \overline{Mn}(PPh_3) + MeCN \qquad (11)$$

identified positively by its characteristic infrared spectrum in >95% yield. Similarly, $\overline{Mn}(py)$ could be completely converted to the phosphine analogue $\overline{Mn}(PPh_3)$ by catalytic amounts of the cation $\overline{Mn}(py)^+$, without the continued passage of current.

The ease with which the catalytic ligand substitution can be chemically initiated (as in eq 11) depends on the reduction potential of $\overline{Mn}L$. Thus it may even be induced adventitiously when a readily oxidized manganese carbonyl such as $\overline{Mn}(NCMe)$ or $\overline{Mn}(py)$ is exposed to air.[29]

Discussion

Ligand substitution in its most general form represents an exchange process such as

$$\overline{Mn}L + \boldsymbol{L} \rightleftharpoons \overline{Mn}\boldsymbol{L} + L \qquad (12)$$

The notation $\overline{Mn}$ in eq 12 designates the carbonylmanganese moiety $(\eta^5\text{-}C_5H_4Me)Mn(CO)_2$ used in this study, and L and **L** represent the displaced and substituting ligands, respectively. Electrocatalysis of ligand substitution thus refers to the promotion of eq 12 at an electrode with minimal consumption of current, under conditions in which the conventional thermal process is either nonexistent or unimportant. Since the electrochemically induced process is truly catalytic, the electrode only facilitates the *rate* of ligand substitution and does not alter the *position* of the equilibrium in eq 12.

I. Catalytic Cycles for Ligand Substitution by Radical Chain Processes. We show how the well-behaved electrochemical characteristics of the series of manganese carbonyls $\overline{Mn}L$ allow us to establish the kinetics and mechanism of electrocatalysis for

(27) For example, bulk electrolysis at 22 °C resulted in the complete destruction of the carbonylmanganese moiety (as monitored by IR spectrophotometry), and it was accompanied by the evolution of CO. Such a lability of $\overline{Mn}L^+$ is not inconsistent with the reversible oxidations observed by cyclic voltammetry, since a half-life of the order of seconds is sufficient to yield i_p^a/i_p^c of unity.[28]

(28) Nicholson, R. S.; Shain, I. *Anal. Chem.* **1964**, *36*, 706.

(29) For example, when an acetone solution of $\overline{Mn}(py)$ and PPh_3 was stirred for 5 min under a blanket of oxygen at room temperature, IR analysis showed a 50% conversion to $\overline{Mn}(PPh_3)$. Considerable loss of manganese complex arising from destructive oxidation also occurred. See also ref 6.

Scheme I

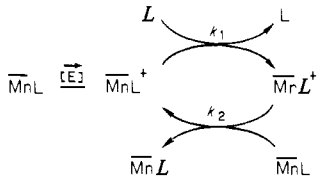

Scheme II

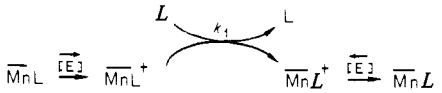

the ligand substitution process in considerable, quantitative detail. We begin the discussion by emphasizing the high turnover numbers in excess of 1000 that can be achieved for electrocatalysis. As such, the chain substitution can be triggered by either a direct chemical (eq 11) or an electrochemical (eq 3) method of initiation.

$$\text{initiation} \qquad \overline{\text{Mn}}\text{L} \overset{[\bar{E}]}{\rightleftharpoons} \overline{\text{Mn}}\text{L}^+ + \text{e} \qquad (13)$$

Indeed, the anode provides an unique device for continuously generating the active species, which is readily identified by both transient and bulk electrochemical methods as the metastable 17-electron cation radical. The propagation steps for the catalytic chain process stem from the enhanced rates of ligand substitution, which we have established in eq 8 and 9 for such cations:

$$\text{substitution} \qquad \overline{\text{Mn}}\text{L}^+ + \boldsymbol{L} \overset{k_1}{\rightleftharpoons} \overline{\text{Mn}}\boldsymbol{L}^+ + \text{L} \qquad (14)$$

The propagation sequence is completed by the electron transfer process in eq 15.

$$\text{electron transfer} \qquad \overline{\text{Mn}}\boldsymbol{L}^+ + \text{MnL} \overset{k_2}{\rightleftharpoons} \overline{\text{Mn}}\boldsymbol{L} + \overline{\text{Mn}}\text{L}^+ \qquad (15)$$

Substitution and electron transfer in eq 14 and 15 together represent the minimum number of discrete steps to constitute the catalytic cycle required for the overall stoichiometry in eq 12. Such a chain mechanism for electrocatalysis is schematically represented in Scheme I. This formulation emphasizes the equivalence between the electrode-mediated and the chemically induced methods for the initiation of the electrocatalysis. If substitution and electron transfer in eq 14 and 15 are both efficient, Scheme I predicts the occurrence of electrocatalytic processes with high turnover numbers.[30] However, it is important to note that the reduction potential $E°$ of the product $\overline{\text{Mn}}\boldsymbol{L}^+$ in eq 14 is more positive than the potential [E] at which the electrocatalysis is effectively initiated. Accordingly, it is also possible for the catalytic cycle to be completed by back electron transfer at the electrode potential [E]:

$$\overline{\text{Mn}}\boldsymbol{L}^+ + \text{e} \xrightarrow{[\bar{E}]} \overline{\text{Mn}}\boldsymbol{L} \qquad (16)$$

Under these circumstances, an alternative mechanism exists in which the electrocatalysis is strongly mediated by the electrode (Scheme II). This electrocatalytic process will be particularly beneficial for those ligand substitutions with short kinetic chain lengths, since the current efficiency will not be critically dependent on the facility of the electron transfer step in eq 15.

The essential difference between the mechanisms in Schemes I and II resides in the pathways by which electron transfer to the cationic product $\overline{\text{Mn}}\boldsymbol{L}^+$ is effected. In Scheme I, electron transfer by eq 15 is a homogeneous process, whereas in Scheme II it occurs at an electrode surface (eq 16). Since both processes are likely to be outer-sphere electron transfers, they are expected to be highly competitive.[31] Indeed the partitioning between homogeneous and heterogeneous electron transfer represents a characteristic ambiguity in many electrochemical ECE processes.[32-39] Accordingly, let us consider the kinetics of electrocatalysis using the generalized Scheme III for the ECE process that is applicable to ligand substitution.

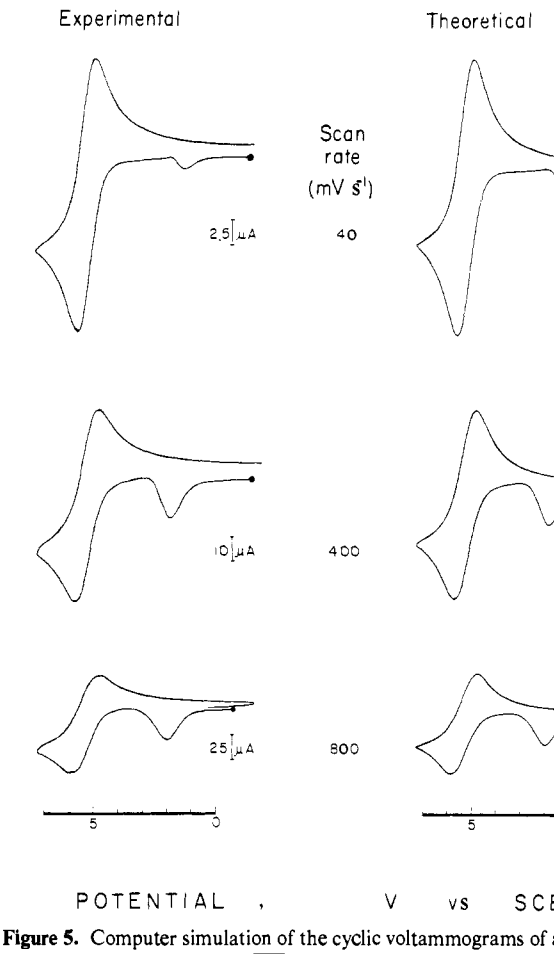

Figure 5. Computer simulation of the cyclic voltammograms of a solution containing 1.04×10^{-3} M $\overline{\text{Mn}}$(NCMe) and 2.94×10^{-3} M PPh_3 in acetonitrile containing 0.1 M TEAP at the various scan rates indicated. See Experimental Section for the details of the optimum parameters used in the simulation.

Scheme III

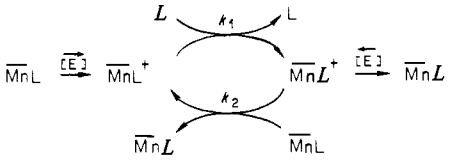

II. Kinetics of the Electrocatalytic Ligand Substitution by Digital Simulation. The kinetics for Scheme III can be immediately simplified by first focussing on the ligand substitution $\overline{\text{Mn}}$(NCMe) by PPh_3 in eq 10. In this system, the ligand exchange step in eq 17 and the electron-transfer step in eq 18 are

(30) The current efficiency generally increases with the concentration function [ML][L], which is consistent with chain termination via a first-order decomposition of ML^+ and/or ML^+.

(31) For a discussion of heterogeneous and homogeneous electron transfer by an outer-sphere mechanism for a common series of electron donors, see: Klingler, R. J.; Kochi, J. K. *J. Am. Chem. Soc.* **1981**, *103*, 5839.

(32) "ECE" refers to a scheme involving an initial electrode process followed by a chemical reaction to form a new electroactive species.

(33) Hawley, M. D.; Feldberg, S. W. *J. Phys. Chem.* **1966**, *70*, 3459.

(34) Saveant, J. M. *Acc. Chem. Res.* **1980**, *13*, 323.

(35) (a) Feldberg, S. W. *J. Phys. Chem.* **1971**, *75*, 2377. (b) Feldberg, S. W.; Jeftic, L. *Ibid.* **1972**, *76*, 2439.

(36) Bond, A. M.; Darensbourg, D. J.; Mocellin, E.; Stewart, B. J. *J. Am. Chem. Soc.* **1981**, *103*, 6827.

(37) (a) Bond, A. M.; Grabaric, B. S.; Jackowski, J. J. *Inorg. Chem.* **1978**, *17*, 2153. (b) Bond, A. M.; Colton, R.; Jackowski, J. J. *Ibid.* **1975**, *14*, 274.

(38) Amatore, C.; Pinson, J.; Saveant, J. M.; Thiebault, A. *J. Electroanal. Chem. Interfacial Electrochem.* **1980**, *107*, 59, 75.

(39) (a) Amatore, C.; Pinson, J.; Saveant, J. M.; Thiebault, A. *J. Am. Chem. Soc.* **1982**, *104*, 817. (b) *Ibid.* **1981**, *103*, 6930.

$$\overline{Mn}(NCMe)^+ + PPh_3 \rightarrow \overline{Mn}(PPh_3)^+ + MeCN \quad (17)$$

$$\overline{Mn}(PPh_3)^+ + \overline{Mn}(NCMe) \rightarrow \overline{Mn}(PPh_3) + \overline{Mn}(NCMe)^+ \quad (18)$$

both essentially irreversible—the first owing to the absence of the reverse step as shown by cyclic voltammetry,[40] and the second arising from the large separation in the reduction potentials $E°$ for $\overline{Mn}(NCMe)^+$ and $\overline{Mn}(PPh_3)^+$ in Table I.

Digital simulation of the cyclic voltammogram of $\overline{Mn}(NCMe)$ in the presence of added PPh_3 was carried out by using the method of finite differences, as described by Feldberg.[41,42] Accurate simulation requires a knowledge of $E°$ for $\overline{Mn}(NCMe)$ and $\overline{Mn}(PPh_3)$ as well as their intrinsic heterogeneous rate constants k_s and diffusion coefficients D, which can be determined by the independent procedures described in the Experimental Section.[43] Thus our immediate goal is to substantiate the kinetic form of Scheme III and to determine the homogeneous kinetic parameters k_1 and k_2 in eq 14 and 15, respectively.

Figure 5 (left side) illustrates how the cyclic voltammogram of $\overline{Mn}(NCMe)$ is affected by the presence of PPh_3 at different CV sweep rates. The values of the rate constants k_1 and k_2 were determined by an iterative procedure in which a value of k_2 was arbitrarily selected at first and the value of k_1 varied until the match of the simulated and experimental cyclic voltammograms was optimized. The procedure was repeated until successful simulation was achieved, with $k_1 = 1.3 \times 10^4$ M^{-1} s^{-1} and $k_2 = 5 \times 10^5$ M^{-1} s^{-1}, as shown by the comparison of the theoretical cyclic voltammograms on the right side of Figure 5. The sensitivity of the simulated cyclic voltammograms to the choice of k_1 and k_2, as well as the other electrochemical parameters, is described further in the Experimental Section. Suffice it to mention here that such an optimization of the computer-simulated cyclic voltammogram is not critically dependent on the value of k_2 if it is chosen over the range $10^4 < k_2 < \infty$[44] for scan rates between 40 and 800 mV s^{-1}. By contrast, the manifestation of the reactant wave (particularly the anodic peak current i_p^a) is quite sensitive to the value of k_1. As a result, values of k_1 can be evaluated with a precision of better than 15% by a straightforward comparison of the simulated and experimental cyclic voltammograms.[45] Importantly, the reliability of these computed values of k_1 and k_2 is further shown in Figure 6 by the excellent fit of *all* the simulated cyclic voltammograms to the experimental ones that were obtained by systematically varying the concentrations of PPh_3 and $\overline{Mn}(NCMe)$ over a rather wide range.

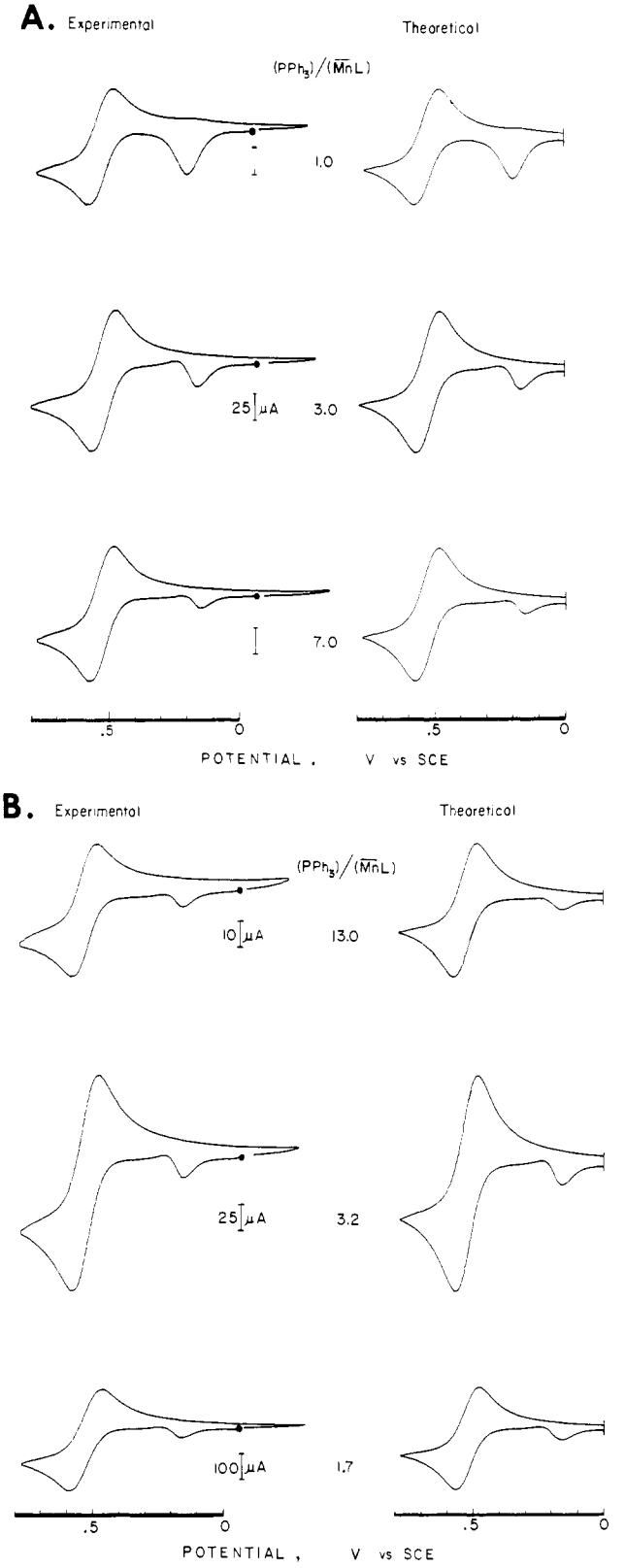

Figure 6. Agreement between the computed and the experimental CV using the same single set of parameters in Figure 5: (A) 1.7×10^{-3} M $\overline{Mn}(NCMe)$ with varying molar ratios of PPh_3, as indicated; (B) 1.0×10^{-2} M PPh_3 and varying molar ratios of $\overline{Mn}(NCMe)$, as indicated. All CVs recorded in acetonitrile containing 0.1 M TEAP at 22 °C and a scan rate of 400 mV s^{-1}.

III. Rate Constants and Mechanisms for Ligand Substitution of Cationic $\overline{Mn}L^+$ Intermediates. We conclude from the CV simulation studies that the overall rate of electron transfer, including both homogeneous and heterogeneous components in eq

(40) Thus the CV of $\overline{Mn}(PPh_3)$ in acetone is unaffected by the presence of MeCN in high concentrations.

(41) Feldberg, S. W. In "Electroanalytical Chemistry"; Bard, A. J., Ed.; Dekker: New York, 1969; Vol. 3, p 199, and In "Computer Applications in Analytical Chemistry"; Mark, H. B., Ed.; Dekker: New York, 1972; p 185.

(42) Owing to long kinetic chain lengths extant in our system, termination processes were not required for the accurate simulation of the cyclic voltammograms. By contrast, compare the systems in ref 38 and 39.

(43) The transfer coefficient β is also required for simulation although the calculated voltammograms are rather insensitive to this parameter (see Experimental Section). The effect of the transfer coefficient on cyclic voltammetry is discussed in ref 24.

(44) The upper limit exceeds the diffusion-controlled rate.

(45) We cannot determine the electron-transfer rate constant accurately because the theoretical voltammograms are insensitive to the value of k_2. This facet may be illustrated by a simple analysis of the kinetics of Scheme III, in which the steady-state concentration of the substituted radical is given by $[\overline{Mn}L^+] = (k_1/k_2)[\overline{Mn}L^+][L]/[\overline{Mn}L]$. Upon the application of the Nernst equation, the rate of product formation is $d[\overline{Mn}L]/dt = k_1 \exp[(n\mathcal{F})(RT)^{-1}(E - E^0)][\overline{Mn}L][L]$, which is only a function of k_1 and E. Therefore if $\overline{Mn}L^+$ is a transient intermediate (as opposed to being the product), the ligand substitution (i.e., k_1 in eq 14) is the rate-limiting process. [In fact, the computational function of k_2 is to keep the concentration of $\overline{Mn}(PPh_3)^+$ near zero until $\overline{Mn}(NCMe)$ is depleted—which is a restatement of the kinetic observation that the ligand substitution step in eq 18 is rate limiting.] The calculation of k_2 by the Marcus cross relationship using the measured values of k_s and $E°$ [35b] affords rates that are slightly too slow. Preliminary results suggest k_2 calculated by the Rehm–Weller expression (see ref 31) afford more consistent values (unpublished results).

15 and 16, is fast compared to the rate of the ligand exchange step in eq 14. As such, we now inquire about the nature of the rate-limiting exchange step itself since there are two important possibilities, viz., an associative or a dissociative mechanism.[46]

In the digital simulation of the cyclic voltammograms, the ligand exchange reaction in eq 14 has been implicitly formulated as a one-step, bimolecular substitution reaction. The kinetics of this *associative* process are given by the second-order rate expression:

$$-\frac{d[\overline{Mn}L^+]}{dt} = k_1[\overline{Mn}L^+][L] \qquad (19)$$

The dissociative counterpart to this mechanism is represented as a two-step process:

$$\overline{Mn}L^+ \underset{k_{-3}}{\overset{k_3}{\rightleftharpoons}} \overline{Mn}^+ + L \qquad (20)$$

$$\overline{Mn}^+ + L \xrightarrow{k_4} \overline{Mn}L^+ \qquad (21)$$

For this *dissociative* mechanism, the general rate expression employing the steady-state approximation is given as

$$-\frac{d[\overline{Mn}L^+]}{dt} = \frac{k_3k_4[\overline{Mn}L^+][L]}{k_{-3}[L] + k_4[L]} \qquad (22)$$

for which two limiting kinetic extremes can be considered. First, for a rate-determining dissociation of the ligand L, i.e., $k_{-3}[L] << k_4[L]$, the first-order rate expression is independent of nucleophile L. This kinetic description is clearly not compatible with the results in Figure 6, which shows a marked dependence on PPh_3. Second, the other kinetic extreme of $k_{-3}[L] >> k_4[L]$ is described by the rate expression

$$-\frac{d[\overline{Mn}L^+]}{dt} = \frac{k_3k_4[\overline{Mn}L^+][L]}{k_{-3}[L]} \qquad (23)$$

The rate of such a reversible dissociative process is only distinguished from the associative process by an inverse dependence on the concentration of the departing ligand L. Since acetonitrile is the solvent as well as the departing ligand, we repeated the cyclic voltammetry of $\overline{Mn}(NCMe)$ and PPh_3 in an acetone medium. Simulation of the cyclic voltammogram obtained under these conditions afforded the exchange rate constant k_1 as 3.3×10^3 M^{-1} s^{-1}, which is actually a factor of less than 4 slower than the value in acetonitrile. To eliminate any ambiguity arising from solvent effects, we also found that the cyclic voltammogram of $\overline{Mn}(NCMe)$ and PPh_3 in acetone was singularly unchanged in the presence of a 100-fold excess of acetonitrile.[47] In a similar way, the cyclic voltammogram of $\overline{Mn}(py)$ and PPh_3 is unaffected by as much as a 100-fold excess of added pyridine. Thus we conclude that the reversible dissociative mechanism in eq 20 and 21 does not play a significant role in the ligand exchange step.

The associative mechanism for the ligand exchange step in eq 17 is also favored by an analysis of the activation parameters. The experimental data consisted of a series of cyclic voltammograms recorded at temperatures varying incrementally from −40 to 25 °C. [The digital simulation technique for the evaluation of k_1 included the temperature variation of the diffusion coefficient, as described in the Experimental Section.] The remarkably linear Arrhenius plot of the exchange rate constant (log k_1) in Figure 7 afforded the activation parameters $\Delta H^\ddagger = 4.4$ kcal mol^{-1} and $\Delta S^\ddagger = -25$ eu. Indeed, the negative entropy of activation readily accords with the associative mechanism proposed for the ligand exchange process.[48]

The successful evaluation of the rapid rates of ligand exchange by the computer simulation of the cyclic voltammograms enabled us to determine the structural effects of the substituting nucleophile L and of the displaced ligand L on the exchange rate constant

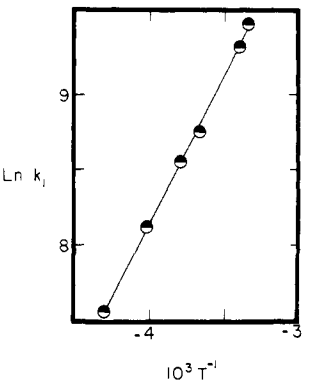

Figure 7. Temperature variation of the second-order rate constant k_1 for the ligand substitution of the 17-electron cationic $\overline{Mn}(NCMe)^+$ by PPh_3 in acetonitrile containing 0.1 M TEAP.

Table III. Second-Order Rate Constants k_1 for the Ligand Exchange of the 17-Electron Cationic $\overline{Mn}L^+$ by the Added Nucleophiles L[a]

L	L	solvent	k_1, M^{-1} s^{-1}
MeCN	PPh_3	MeCN	1.3×10^4
MeCN	PPh_3	Me_2CO	3.3×10^3
MeCN	$P(OPh)_3$	MeCN	1.2×10^1
MeCN	$P(Me)Ph_2$	MeCN	$(>10^5)$
MeCN	$P(OMe)Ph_2$	MeCN	2.5×10^4
MeCN	$P(C_6H_4Cl\text{-}p)_3$	MeCN	9.5×10^2
MeCN	$P(C_6H_4Me\text{-}p)_3$	MeCN	3.0×10^4
NC_5H_5(py)	PPh_3	Me_2CO	5.0
NC_5H_5(py)	PEt_3	Me_2CO	1.3×10^3

[a] At 25 °C in solutions containing 0.1 M tetraethylammonium perchlorate as supporting electrolyte and to maintain constant ionic strength.

k_1 for the cationic $\overline{Mn}L^+$. It is noteworthy that the second-order rate constants k_1 listed in Table III span a range of more than 10^4 M^{-1} s^{-1} with only minor changes in L and L.[49] In order to substantiate the reliability of the absolute rate constants determined by the digital simulation technique, we independently measured the relative rate constants by the competition method. Thus the electrocatalytic substitution of $\overline{Mn}(NCMe)$ was carried out in a solution containing a stoichiometric excess of two nucleophiles L and L'.[50] The pertinent competition in the substitution step is

$$\overline{Mn}(NCMe)^+ + L \xrightarrow{k_1} \overline{Mn}L^+ + MeCN \qquad (24a)$$

$$\overline{Mn}(NCMe)^+ + L' \xrightarrow{k_1} \overline{Mn}L'^+ + MeCN \qquad (24b)$$

The approximate zero-order dependence on the nucleophiles allows the relative rate constants k_1/k_1' to be evaluated from the quantitative analysis of the products $\overline{Mn}L$ and $\overline{Mn}L'$ by infrared spectrophotometry as

$$\frac{k_1}{k_1'} \simeq \frac{[\overline{Mn}L][L']}{[\overline{Mn}L'][L]} \qquad (25)$$

The agreement between computational results of the digital simulation and the competition method is quite satisfactory. For example, in the nucleophile pair $P(C_6H_4Cl\text{-}p)_3/P(OPh)_3$, the rate ratios k_1/k_1' were found to be 79 and 89 by digital simulation and competition, respectively.[51] Similarly, for the nucleophile

(46) For a discussion of associative and dissociative mechanisms in ligand substitution, see: Langford, C. H.; Gray, H. B. "Ligand Substitution Processes"; Benjamin: New York, 1965.

(47) The absolute concentration of ca. 0.2 M for MeCN in these experiments is sufficiently low so as not to affect the solvent properties.

(48) For a discussion, see ref 3a, pp 129, 474–477.

(49) The detailed evaluation of leaving-group and entering-group effects in ligand substitution will be reported in a separate study.

(50) (a) Under the conditions of the competition experiments, phosphine scrambling in the substitution products ML and ML' is minor. (b) In these systems, the electron-transfer rate constants k_2 and k_2' are much faster than the ligand-exchange rate constants k_1 and k_1'.

(51) The discrepancy may be partly attributed to the high concentration (~0.2 M) of $P(OPh)_3$, which causes deviation from its thermodynamic activity. Furthermore, small amounts of CH_2Cl_2 (20 %v) were used in the competition experiments as a cosolvent.

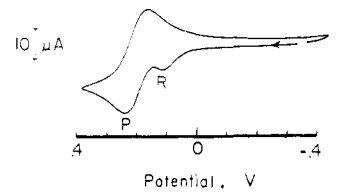

Figure 8. Cyclic voltammogram of a solution of $\sim 10^{-3}$ M $\overline{Mn}(py)$ in acetonitrile containing 0.1 M TEAP at 25 °C and a scan rate of 50 mV s^{-1}. Note the minor contribution of the reactant $\overline{Mn}(py)$ R relative to the ligand substitution product $\overline{Mn}(NCMe)$ P.[61]

pair $PPh_3/P(C_6H_4CH_3\text{-}p)_3$, the rate ratios k_1/k_1' were evaluated as 0.43 and 0.49 by digital simulation and competition, respectively.[52]

The second-order rate constants k_1 for the ligand substitution of the 17-electron carbonylmanganese cations in Table III are unusual for several reasons. First, the absolute magnitudes of the rate constants are much larger than those commonly encountered in their diamagnetic counterparts.[53,54] Second, the sensitivity of the rate constant to the structural effects of the incoming nucleophile *L* is unusually high. For example, PPh_3 is more than 10^3 times as reactive as $P(OPh)_3$, whereas in other systems the factor is usually much less.[55,56] Moreover, the trend in the reactivity of a triad of related triarylphosphine nucleophiles, (viz., triphenylphosphine, tri-*p*-tolylphosphine, and tri(*p*-chlorophenyl)phosphine) toward ligand substitution of $\overline{Mn}(NCMe)^+$ coincides closely to that trend observed in the nucleophilic substitution of benzyl chloride.[57] (Note the latter represents a classical example of a bimolecular S_N2 substitution.[58]) Such structural effects on the rate are much more attenuated in other systems. The lability of the leaving ligand is also highly magnified in $\overline{Mn}L^+$, as shown by the factor of $\sim 10^3$ that separates L = MeCN from L = pyridine, when PPh_3 is the nucleophile in an acetone medium.[59] Finally, it must be emphasized that the associative process dominates the ligand substitution in $\overline{Mn}L^+$ and any contribution from a dissociative process must minor.[60] This highly unusual mechanistic dichotomy for ligand substitution in the 17-electron carbonylmetal cation merits further attention.[4a]

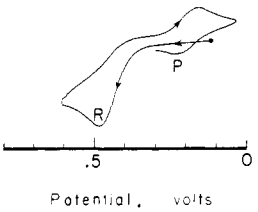

Figure 9. Initial positive scan CV of 1.0×10^{-3} M $\overline{Mn}$(norbornene) R in acetonitrile containing 0.1 M TEAP at 22 °C and a scan rate of 500 mV s^{-1}. Note the appearance of the reversible wave due to $\overline{Mn}(NCMe)$ P on the return scan.

IV. Thermodynamics of the Catalytic Ligand Substitution. In the foregoing section, we showed how the *kinetics* of each step in the catalytic cycle for ligand substitution can be determined. Let us now consider how the *thermodynamic driving force* for each step in the radical chain process can be measured. We begin by noting in Figure 8 that the cyclic voltammogram of $\overline{Mn}(py)$ in acetonitrile consists mainly of a reversible wave owing to the substitution product $\overline{Mn}(NCMe)$ P, together with only a minor wave of $\overline{Mn}(py)$ R.[61] The reverse process is also observed, albeit less dramatically, in the CV oxidation of $\overline{Mn}(NCMe)$ in acetonitrile solution containing pyridine (10% v/v) by the exaggerated separation of the anodic (E_p^{ox}) and cathodic (E_p^{red}) waves. These observations lead to the conclusion that ligand exchange in eq 26

$$\overline{Mn}(py) + MeCN \underset{|E|}{\overset{K_{eq}}{\rightleftharpoons}} \overline{Mn}(NCMe) + py \qquad (26)$$

proceeds readily in both directions. The equilibrium condition in eq 26 was evaluated quantitatively by the electrostimulation of an acetone solution of $\overline{Mn}(py)$ and acetonitrile, followed by the quantitative analysis of $\overline{Mn}(NCMe)$ and $\overline{Mn}(py)$ by IR spectrophotometry. Similarly, the microscopic reverse process was examined by the electrostimulation of $\overline{Mn}(NCMe)$ in the presence of various amounts of pyridine and acetonitrile, as described in the Experimental Section. (In each case, the current efficiencies of the catalytic ligand exchange as measured by coulometry always exceeded 20.) The equilibrium constant of $K_{eq} = 1.1 \pm 0.1 \times 10^{-2}$ was found to be independent of the initial conditions, and it corresponds to an overall free energy change of $\Delta G = 2.6$ kcal mol^{-1} for eq 26.

The electron-transfer step in the catalytic cycle is given by

$$\overline{Mn}(NCMe)^+ + \overline{Mn}(py) \rightleftharpoons \overline{Mn}(NCMe) + \overline{Mn}(py)^+ \qquad (27)$$

for which the free energy change may be evaluated from the formal reduction potentials $E°$ of $\overline{Mn}(NCMe)^+$ and $\overline{Mn}(py)^+$. The values of $E°$ are well approximated by the reversible CV peak

(52) Owing to small shifts in ν(CO) for $\overline{Mn}(PPh_3)$ relative to that of $\overline{Mn}[P(C_6H_4Cl\text{-}p)_3]$, there is an experimental uncertainty of $\sim\pm 50\%$ in these values.

(53) Mononuclear octahedral metal carbonyls are generally inert toward substitution, except at elevated temperatures. Associative and dissociative substitution pathways are extant, although the latter usually dominates. See ref 3b for a review.

(54) Basolo and co-workers have observed the bimolecular CO substitution by phosphines of less than six coordinate complexes. Rate constants near room temperature range up to 10^{-3} M^{-1} s^{-1}. See: (a) Thorsteinson, E. M.; Basolo, F. *J. Am. Chem. Soc.* **1966**, *88*, 3929. (b) Morris, D. E.; Basolo, F. *Ibid.* **1968**, *90*, 2531. (c) Schuster-Woldan, H. G.; Basolo, F. *Ibid.* **1966**, *88*, 1657. (d) Wawersik, H.; Basolo, F. *Ibid.* **1967**, *89*, 4626. (e) See also: Cardaci, G.; Murgia, S. M. *J. Organomet. Chem.* **1970**, *25*, 483.

(55) The relative reactivities of PPh_3 and $P(OPh)_3$ as entering ligands in bimolecular substitutions have been compared for a number of metal carbonyls. Although PPh_3 is almost always more reactive than $P(OPh)_3$, the ratio $k(PPh_3)/k(P(OPh)_3)$ is uniformly less than 10^2. See: (a) ref 54. (b) Angelici, R. J.; Graham, J. R. *J. Am. Chem. Soc.* **1966**, *88*, 3658. (c) Ingemanson, C. M.; Angelici, R. J. *Inorg. Chem.* **1968**, *7*, 2646. (d) Covey, W. D.; Brown, T. L. *Ibid.* **1973**, *12*, 2820. (e) Pöe, A.; Twigg, M. V. *Ibid.* **1974**, *13*, 1860. (f) Ellgen, P. C.; Gerlach, J. N. *Ibid.* **1973**, *12*, 2526. (g) Hart-Davis, A. J.; White, C.; Mawby, R. J. *Inorg. Chim. Acta* **1970**, *4*, 441. (h) Cobb, M. A.; Hungate, B.; Pöe, A. *J. Chem. Soc., Dalton Trans.* **1976**, 2226. (i) Rossetti, R.; Gervasio, G.; Stanghellini, P. L. *Ibid.* **1978**, 222.

(56) Covey and Brown[55d] have suggested that coordinatively saturated metal carbonyls undergo bimolecular displacement by a dissociative interchange (I_d) mechanism. This follows from the insensitivity of reaction rates to the structure of the entering ligand and the general occurrence of a competing dissociative pathway. See ref 46 for a general discussion of interchange mechanisms.

(57) McEwen and co-workers have reported the rate constants for the reactions of PPh_3 and $P(C_6H_4Me\text{-}p)_3$ (and many other triarylphosphines) with benzyl chloride at 31 °C in a 3:2 mixture of benzene and methanol. The rate constant for $P(C_6H_4Cl\text{-}p)_3$, obtained by extrapolation of a Hammett correlation using $\sum\sigma_{para}$, is 1.07×10^{-2} M^{-1} s^{-1}. The plot of log [k($PhCH_2Cl$)] vs. log [$k(\overline{Mn}(NCMe)^+)$] for the three phosphines is approximately linear with a least-squares slope of ~ 0.9. See: McEwen, W. E.; James, A. B.; Knapczyk, J. W.; Kyllingstad, V. L.; Shiav, W. S.; Shore, S.; Smith, J. H. *J. Am. Chem. Soc.* **1978**, *100*, 7304.

(58) For a discussion of the nucleophilic substitution of benzyl halides, see: (a) Streitwieser, A., Jr. "Solvolytic Displacement Reactions"; McGraw-Hill: New York, 1962; pp 18–20. (b) Shiner, V. J., Jr. In "Isotope Effects in Chemical Reactions"; Collins, C. J., Bowman, N. S., Ed.; Van Nostrand Reinhold: New York, 1970; pp 115–118.

(59) For example, the upper rate limit for py dissociation from $\overline{Mn}(py)^+$ in acetone at 25 °C is ca. 10^{-3} s^{-1}, on the basis of reversible cyclic voltammetric oxidation of $\overline{Mn}(py)$ (see the treatment of Nicholson and Shain in ref 28 for the kinetics of EC processes). Thus the value of k_1 for the reaction of $\overline{Mn}(py)^+$ with PEt_3 in acetone (1.3×10^3 M^{-1} s^{-1}) indicates an enormous increase in the rate of loss of py induced by added phosphine.

(60) (a) It is conceivable that an undetected, slow dissociation pathway might be important at lower concentrations of $\overline{Mn}L$ and *L* than could be employed in this study. (b) An alternative quasi-dissociative mechanism involves a preequilibrium requiring an intermediate with a lowered hapticity of the cyclopentadienyl ring (see: Wegman, R. W.; Brown, T. L. *Organometallics* **1982**, *1*, 47, for a notable example). However, the constancy of k_1 over a 10-fold range in the concentration of *L* (vide supra) militates against this formulation.

(61) The large shift of E_p^{ox} for $\overline{Mn}(py)$ to more negative potentials in Figure 8 is a kinetic phenomenon and is predictable on the basis of digital simulations. See, for example: Figures 5 and 6 for the negative shift of E_p^{ox} of $\overline{Mn}(NCMe)$ induced by PPh_3.

potentials (i.e., $E^\circ \simeq (E_p^{ox} + E_p^{red})/2$),[62] which are listed in Table II, entries 2 and 3. Accordingly, we proceed from the Nernstian relationship to calculate the driving force for the electron-transfer step in eq 27 to be −0.19 kcal mol^{-1}. Since the ligand exchange step in eq 28 simply represents the algebraic difference of the

$$\overline{Mn}(py)^+ + MeCN \rightleftharpoons \overline{Mn}(NCMe)^+ + py \qquad (28)$$

equilibria in eq 26 and 27, it follows that the free energy change for the exchange step in eq 28 is 2.8 kcal mol^{-1}.

In the foregoing example, the thermodynamics for the overall ligand substitution in eq 26 is largely determined by the driving force for the cation exchange in eq 28, since the electron-transfer step in eq 27 is close to being isoergonic. Moreover, the facile substitution of the nitrogen-centered ligands by phosphines cited in Table I derives from catalytic cycles in which both steps are quite exergonic.[63] Let us now consider the substitution of $\overline{Mn}$(norbornene) by acetonitrile in which the electron-transfer step

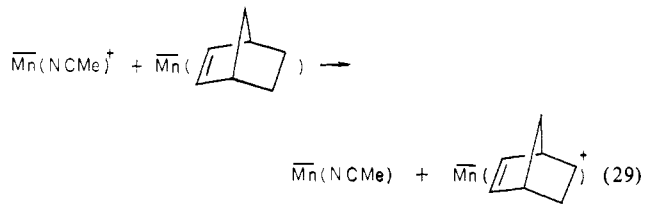

is endergonic endergonic (ΔG = 5.72 kcal mol^{-1}). Cyclic voltammetry indicates that the ligand exchange step does occur in the cation,

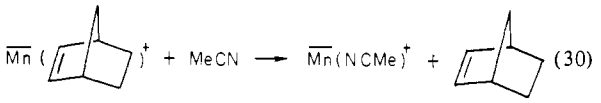

since the reversible CV wave of $\overline{Mn}$(NCMe) is readily observed on the return sweep from the anodic oxidation of $\overline{Mn}$(norbornene) in acetonitrile as shown in Figure 9. Furthermore, it can be demonstrated independently that the equilibrium for the overall ligand substitution process in eq 31 lies to the right.[64] Nonetheless,

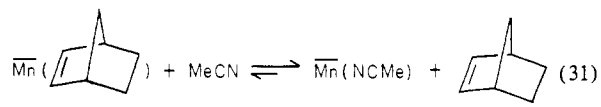

the electroxidation of an acetonitrile solution of $\overline{Mn}$(norbornene) resulted in only a 21% conversion and a 15% yield of $\overline{Mn}$(NCMe),[65] with an overall current efficiency of 2. Under these circumstances, the inefficiency of the electrocatalytic ligand substitution is most simply attributed to the endergonicity of the electron-transfer step in eq 29.[66]

Summary and Conclusions

The radical chain mechanism for the ligand substitution of various carbonylmanganese derivatives $\overline{Mn}$L by added nucleophiles *L* in eq 12 has been established to proceed rapidly, and with high efficiency, under conditions in which the more conventional thermal process is too slow to be observed. Chain initiation can be effected chemically or at an electrode surface. Indeed, bulk and transient electrochemical methods provide a quantitative means of establishing the kinetics, the thermodynamics, and the detailed mechanism for the catalytic ligand substitution.

The key features of the radical chain mechanism are (1) initiation by oxidation of the carbonylmetal $\overline{Mn}$L to the 17-electron cation $\overline{Mn}L^+$ by either a chemical oxidant or at the anode [Ē] in eq 13, (2) rapid ligand exchange of the paramagnetic intermediate $\overline{Mn}L^+$ with the added nucleophile *L* to afford the cationic product $\overline{Mn}L^+$ in eq 14, (3) facile reduction of $\overline{Mn}L^+$ by $\overline{Mn}$L in eq 15 and/or at the electrode in eq 16. Such a catalytic process is readily apparent in the cyclic voltammograms of various mixtures of $\overline{Mn}$L and *L* in which the rapid disappearance of $\overline{Mn}$L and concomitant appearance of $\overline{Mn}L$ are apparent, at even the fastest sweep rates. Indeed, digital simulation of the experimental cyclic voltammograms in Figures 5 and 6 establish the kinetics of the catalytic cycle, as described by the elementary steps in eq 13–16 (see Scheme III). The matching of the theoretical to the experimental peak currents of the anodic wave of $\overline{Mn}$L in the presence of *L* is especially useful for providing a quantitative measure of the rate of the cation substitution in eq 14. The digital simulation of the cyclic voltammograms demonstrates that the ligand substitution proceeds by second-order kinetics, with a rate constant k_1, which can easily exceed 10^4 M^{-1} s^{-1}. The validity of the digital simulation method for the determination of k_1 can be independently verified by competition experiments utilizing pairs of added nucleophiles *L*. Structural effects of *L* on the second-order rate constant k_1 are unusually pronounced in this system, in comparison with those previously measured for other carbonylmetals. The associative mechanism proposed for the ligand exchange accords with the activation entropy of $\Delta S = -25$ eu, which has been measured for the reaction of $\overline{Mn}(NCMe)^+$ and PPh_3.

Thermodynamic equilibrium can be established in both the forward and microscopic reverse directions between the pair of carbonylmetals $\overline{Mn}$(NCMe) and $\overline{Mn}$(py) in the presence of py and MeCN, respectively. The evaluation of the equilibrium constant K_{eq} allows the overall driving force for ligand substitution ΔG_{LS} to be established. Moreover, the driving force for the electron-transfer step ΔG_{ET} between $\overline{Mn}(NCMe)^+$ and $\overline{Mn}$(py), and its microscopic reverse, is evaluated from the formal reduction potentials E° of the respective redox couples. The difference represents the driving force ΔG_{LX} for the ligand exchange between the cationic intermediate $\overline{Mn}(NCMe)^+$ and the pyridine nucleophile. The evaluation of the driving force for other catalytic ligand substitutions may be carried out by a similar analysis.

Experimental Section

Materials. Reagent grade acetonitrile (Fisher Scientific) was further purified by distillation from calcium hydride, followed by stirring over a mixture of potassium permanganate and sodium carbonate for 24 h at room temperature. The acetonitrile was distilled at reduced pressure and then redistilled from phosphorus pentoxide. A final fractional distillation from calcium hydride through a 19-plate bubble-cap (Oldershaw) column afforded acetonitrile suitable for electrochemistry. It was stored in a Schlenk flask under argon. Fisher "Spectranalyzed" methylene chloride and acetone were used without further purification. For electrochemical use, tetrahydrofuran (THF) was distilled from lithium aluminum hydride and stored under argon. For most of the preparative reactions, unpurified THF was adequate. Tetraethylammonium perchlorate (TEAP) and tetrabutylammonium perchlorate (TBAP) were used as received from G. F. Smith Chemical Co. (η^5-C_5H_4Me)$Mn(CO)_3$ was obtained from Alfa/Ventron. Triphenylarsine, trimethyl phosphite, and triphenyl phosphite were obtained from Aldrich Chemical Co. Methyldiphenylphosphine was purchased from Organometallics, Inc., and methoxydiphenylphosphine was obtained from Arapahoe Chemicals. Triphenylantimony, tris(*p*-chlorophenyl)phosphine, and tris(*p*-tolyl)phosphine were products of M&T Chemical Co. Triethylphosphine was obtained from Pressure Chemical Co. *tert*-Butyl isocyanide was prepared by a literature method.[67]

(62) For a general treatment of electrochemistry, see: (a) Bard, A. J.; Faulkner, L. R. "Electrochemical Methods"; Wiley: New York, 1980. (b) Pletcher, D. *Chem. Soc. Rev.* **1975**, *4*, 471.

(63) The equilibrium for the overall ligand substitution lies too far to measure accurately.

(64) For example, the ligand substitution in eq 31 may be effected thermally in refluxing acetonitrile solution. Since the reverse ligand substitution (viz., the formation of $\overline{Mn}$(norbornene) from $\overline{Mn}$(NCMe) and norbornene) failed both under thermal as well as electrostimulated conditions, the equilibrium constant $K_{eq} \ll 0$ for eq 31.

(65) When a solution of 0.14 mmol of $\overline{Mn}$(norbornene) in 12 mL of MeCN was electrolyzed at 500 μA for 38 min, a yield of 0.02 mmol of $\overline{Mn}$(NCMe) was found, together with 0.11 mmol of recovered $\overline{Mn}$(norbornene).

(66) This would not be a factor if $\overline{Mn}(NCMe)^+$ were stable. However, there are pathways available for the ready decomposition of $\overline{Mn}(NCMe)^+$, such as the loss of carbon monoxide, to afford products that do not propagate the chain.

Table IV. Characterization of the Various Carbonylmanganese Derivatives $\overline{MnL}$

entry	L	IR[a]	mp, °C[b]	(lit)	elemental analysis for new compound[c]
1	$HN(CH_2)_5$	1929,1860	71–72	(71–73)[68]	
2	NC_5H_5 (py)	1934,1868	72–73	(75)[69]	
3	MeCN	1950,1886	73	(dec)	C, 52.07; H, 4.26; N, 6.34 (theory: C, 51.97; H, 4.36; N, 6.06)
4	PEt_3	1937, 1874	oil[10d]		
5	norbornene	1969,1910	65–66		C, 63.56; H, 6.00 (theory: C, 63.38; H, 6.03)
6	$P(Me)Ph_2$	1940, 1878	57–58	(55–57)[70a]	
7	$P(C_6H_4Me\text{-}p)_3$	1939,1879	184–186		C, 70.38; H, 5.82 (theory: C, 70.44; H, 5.71)
8	PPh_3	1944,1884	118–119	(119–120)[10c]	
9	$CNCMe_3$	1954,1908	53–54.5		C, 57.09; H, 5.78; N, 5.23 (theory: C, 57.15; H, 5.90; N, 5.13)
10	$P(C_6H_4Cl\text{-}p)_3$	1946,1887	156–158		C, 56.10; H, 3.45; Cl, 19.28 (theory: C, 56.20; H, 3.45; Cl, 19.14)
11	$P(OMe)Ph_2$	1944,1884	64–66		C, 62.41; H, 5.16 (theory: C, 62.08; H, 4.96)
12	$P(OMe)_3$	1947,1892	oil[10d]		
13	$P(OPh)_3$	1970,1910	75–77	(75–76)[70b]	
14	CO	2024,1946	oil		
15	THF	1927,1850[d]			
16	$AsPh_3$	1941,1881	117–119	(118–120)[10d]	
17	$SbPh_3$[e]	1940,1884	99–100		C, 57.79; H, 4.19 (theory: C, 57.50; H, 4.08)
18	Me_2SO	1960,1896	64–66	(66)[71]	
19	SO_2	2018, 1976	90 dec	(73)[71]	

[a] Frequencies (cm^{-1}) of CO stretching recorded in *n*-heptane on a Perkin-Elmer 298 spectrophotometer. [b] Melting points are uncorrected. [c] Microanalyses were performed either by Midwest Microlabs, Ltd., Indianapolis, IN, or by Galbraith Laboratories, Inc., Knoxville, TN. [d] The IR spectrum was recorded in THF. [e] The IR spectrum of this compound is reported in ref 72.

The substituted carbonylmanganese complexes, $(\eta^5\text{-}C_5H_4Me)Mn(CO)_2L$, listed in Table IV were prepared from $(\eta^5\text{-}C_5H_4Me)Mn(CO)_2(THF)$, which was generated in situ by the irradiation of a solution of $(\eta^5\text{-}C_5H_4Me)Mn(CO)_3$ in THF under argon. The photochemical reactor consisted of a 300-mL cylindrical flask with a 100-W medium-pressure Hg lamp contained in a quartz immersion well.

All preparative reactions and ligand exchange studies were carried out under either a nitrogen or an argon atmosphere. Benchtop manipulations were performed in Schlenk flasks. Many of the manganese complexes employed in this study are generally air-sensitive, both in the solid state as well as in solutions. In a typical procedure, a solution of 2 g of $(\eta^5\text{-}C_5H_4Me)Mn(CO)_3$ in 300 mL of THF was deaerated and irradiated for 50 min at 0 °C. The IR spectrum of the solution indicated that ~90% of the starting material was converted to $(\eta^5\text{-}C_5H_4Me)Mn(CO)_2(THF)$. One equivalent of the appropriate ligand (L = py, MeCN, piperidine, PPh_3, $P(C_6H_4Me\text{-}p)_3$, $P(C_6H_4Cl\text{-}p)_3$, $P(OMe)_3$, $P(OPh)_3$, PEt_3, $P(Me)Ph_2$, $P(OMe)Ph_2$, $CNCMe_3$, Me_2SO, $AsPh_3$, and $SbPh_3$) was added and the solution stirred for several hours at ambient temperatures. During this period, the deep purple color of the THF complex gave way to the yellow or orange color of the product. The THF was removed at reduced pressure, and the residue was taken up in ethyl ether. (When the product was not soluble in ether, chloroform was employed.) Filtration of the solution followed by crystallization from a mixture of ether and hexane or chloroform and ethanol afforded crystalline products in 30–70% yield. For L = PEt_3 and $P(OMe)_3$, the products were oils, which were purified by chromatography on Florisil according to the literature description.[10d] For L = SO_2, sulfur dioxide gas (1 atm) was bubbled through the solution of $(\eta^5\text{-}C_5H_4Me)Mn(CO)_2(THF)$ in THF with rapid stirring. The reaction was complete at room temperature within a few minutes. Crystallization of the product from a mixture of ether and hexane afforded orange crystals in 53% yield on the basis of $(\eta^5\text{-}C_5H_4Me)Mn(CO)_3$. Since THF is not readily displaced from $(\eta^5\text{-}C_5H_4Me)Mn(CO)_2(THF)$ by norbornene, $(\eta^5\text{-}C_5H_4Me)Mn(CO)_2$(norbornene) was prepared directly by the irradiation of $(\eta^5\text{-}C_5H_4Me)Mn(CO)_3$ (2.0 g) in 300 mL of toluene containing a 20-fold excess of norbornene. The product was purified by crystallization from *n*-heptane and obtained in 59% yield.

Electrochemical Measurements. Electrochemistry was performed with a Princeton Applied Research Model 173 potentiostat equipped with a Model 176 current-to-voltage converter, which provided a feedback compensation for ohmic drop between the working and reference electrodes. The high impedance voltage follower amplifier (PAR Model 178) was mounted external to the potentiostat to minimize the length of the connection to the reference electrode for low-noise pickup. Cyclic voltammetry was performed in a cell designed according to Van Duyne and Reilly.[73] The configuration of this cell is convenient for low-temperature experiments since the lower portion of the cell containing the working solution could be easily submerged in the desired cold bath contained in a Dewar flask. The distance between the Pt electrode and the tip of the salt bridge was less than 2 mm to minimize ohmic drop. The reference electrode was isolated from the cold bath and maintained at room temperature (~25 °C). The voltammograms were recorded on a Houston Series 2000 X–Y recorder. Bulk electrolysis was performed in a three-compartment cell equipped with a Pt–gauze working electrode and a magnetic stir bar for agitation. A sidearm provided an inlet for the inert atmosphere, and another permitted the removal of samples of solution. CV scans were recorded several minutes after agitation to ensure thermal equilibration. Electrode aging was not a serious problem in this study. Between experiments the platinum wire was soaked briefly in concentrated nitric acid, rinsed with distilled water, and dried at 110 °C. The variation in effective electrode area from day to day was less than 10%.

For bulk electrolysis at a controlled potential, the current–time profile was stored in a Princeton Applied Research Model 4102 signal recorder for later output onto the X–Y recorder. The signal recorder was interfaced to a Digital Equipment Corp. PDP 11/23 computer, on which all computations were performed. Voltage–time profiles for electrolysis at a controlled current were recorded manually. For bulk electrolyses that required the intermittent sampling of the anolyte by cyclic voltammetry, a specially constructed cell incorporating an auxiliary Pt microelectrode was employed, as described in detail elsewhere.[74]

Electrocatalysis of Ligand Exchange: Typical Example. The ligand substitution of $(\eta^5\text{-}C_5H_4Me)Mn(CO)_2(NCMe)$ by *tert*-butyl isocyanide is reported in detail as a typical example of the experiments listed in Table I. A sample of $(\eta^5\text{-}C_5H_4Me)Mn(CO)_2(NCMe)$ (110 mg, 0.48 mmol) was added to 12 mL of MeCN containing 0.1 M TEAP under a nitrogen atmosphere in the electrolysis cell. The stirred solution was

(67) Weber, W. P.; Gokel, G. W.; Ugi, I. K. *Angew. Chem., Int. Ed. Engl.* **1972**, *11*, 530. Gokel, G. W.; Widera, R. P.; Weber, W. P. *Org. Synth.* **1976**, *55*, 96.

(68) Strohmeier, V. W.; Guttenberger, J. F. *Z. Naturforsch., B: Anorg. Chem., Org. Chem., Biochem., Biophys.*, **1966**, *18B*, 80.

(69) Strohmeier, V. W.; Gerlach, K. *Z. Naturforsch., B: Anorg. Chem., Org. Chem., Biochem., Biophys.*, **1960**, *15B*, 675.

(70) (a) Brown, D. A.; Lyons, H. J.; Manning, A. R. *Inorg. Chim. Acta* **1970**, *4*, 428. (b) Treichel, P. M.; Douglas, W. H.; Dean, W. K. *Inorg. Chem.* **1972**, *11*, 615.

(71) Strohmeier, V. W.; Guttenberger, J. F.; Popp, G. *Chem. Ber.* **1965**, *98*, 2248.

(72) Manning, A. R. *J. Chem. Soc. A* **1971**, 106.

(73) Van Duyne, R. P.; Reilly, C. N. *Anal. Chem.* **1972**, *44*, 142.

(74) Lau, W.; Huffman, J. C.; Kochi, J. K. *Organometallics* **1982**, *1*, 155.

reduced at −0.5 V vs. saturated NaCl SCE for several minutes to render harmless the traces of impurities that may have resulted from adventitous oxidation. When the cathodic current had fallen below about 10 μA, an aliquot of *tert*-butyl isocyanide (40 mg, 0.48 mmol) was added with the aid of a microsyringe. The electrode potential was maintained at −0.5 V and the solution stirred at room temperature for 1 h in subdued roomlight. A 0.25-mL aliquot of the solution was removed and analyzed by IR spectrophotometry to verify that no reaction had occurred. The solution was then oxidized at a controlled current of 100 μA and the electrode potential monitored. After 21.1 min, the potential increased sharply from about 0.0 to +0.3 V and the oxidation ceased. By this time, the deep yellow color of the starting solution had been replaced by the pale yellow color of the product. The carbonyl stretching frequencies in the IR spectrum of $(\eta^5\text{-}C_5H_4Me)Mn(CO)_2(NCMe)$ shifted from 1932 and 1857 cm^{-1} to 1940 and 1881 cm^{-1}, which corresponded to that of the *tert*-butyl isocyanide complex. The anolyte was transferred to a 25-mL volumetric flask and diluted to volume with a solution of deoxygenated MeCN containing 0.1 M TEAP. The yield of $(\eta^5\text{-}C_5H_4Me)Mn(CO)_2(CNCMe_3)$ was determined by IR spectrophotometry to be 95 ± 7% after correction for sampling. For calibration purposes, the product of the optical path length and the molar absorptivity was evaluated by using solutions of authentic $(\eta^5\text{-}C_5H_4Me)Mn(CO)_2(CNCMe_3)$ in MeCN containing 0.1 M TEAP. The plot of absorbance vs. concentration was linear in the concentration range of interest. The anolyte was diluted with 100 mL of deoxygenated water and the resulting light yellow precipitate isolated by filtration (94 mg, 72% isolated yield). The isolated product was found to be spectroscopically identical with that of authentic $(\eta^5\text{-}C_5H_4Me)Mn(CO)_2(CNCMe_3)$. The melting point of the sample after a recrystallization from hexane was 52–54 °C. Although the substitution products were not isolated in many of the other reactions listed in Table I, they were positively identified by their IR spectra in the working solution by comparison with authentic samples.

The electrode-mediated reactions of $(\eta^5\text{-}C_5H_4Me)Mn(CO)_2(THF)$ were performed in situ without isolation of the THF complex. Thus, $(\eta^5\text{-}C_5H_4Me)Mn(CO)_3$ in THF ca. 0.02 M) was irradiated at 0 °C until its conversion was >80% complete by IR spectrophotometry. The concentration of the resulting THF complex was estimated by the decrease in the concentration of the starting tricarbonyl complex. The deep purple solution could be stored at −78 °C for at least 48 h without significant degradation. Nitrogen was avoided as an inert atmosphere for studies aimed at the reactivity of the THF complex, since the reversible ligand exchange to form $(\eta^5\text{-}C_5H_4Me)Mn(CO)_2(N_2)$ has been reported.[75] An argon atmosphere was rigorously maintained over the stock solution, which is extremely air-sensitive. Aliquots were utilized for the electrochemical study by the addition of sufficient tetrabutylammonium perchlorate to make up a 0.1 M solution.

Determination of an Equilibrium Constant. The value of K_{eq} for eq 26 was determined by the electrode-catalyzed equilibration of solutions of $\overline{Mn}(py)$, $\overline{Mn}(NCMe)$, pyridine, and acetonitrile in acetone containing 0.1 M TEAP at various initial concentrations. The quantity $([\overline{Mn}(NCMe)]/[\overline{Mn}(py)])_{eq}$ was evaluated by IR spectrophotometry as described below, and the quantity $([py]/[NCMe])_{eq}$ was derived algebraically. An example of such a determination follows. A mixture of acetonitrile (0.25 mL, 4.79 mmol), pyridine (9.6 μL, 0.119 mmol), and $(\eta^5\text{-}C_5H_4Me)Mn(CO)_2(NCMe)$ (31.2 mg, 0.135 mmol) was added to 10 mL of acetone containing 0.1 M TEAP under argon at room temperature in an electrolysis cell. Subdued roomlight was employed to avoid the complication of a possible photostationary pseudoequilibrium.[76] An oxidizing current of 200 μA was passed through the solution. The composition of the solution was monitored periodically by IR spectrophotometry and found not to change after 28 min. The quantity $[\overline{Mn}(NCMe)]/[\overline{Mn}(py)]$ was evaluated from the absorbances at 1934 and 1920 cm^{-1} and by utilizing equations

$$A_{1934} = 31.0[\overline{Mn}(NCMe)] + 2.4[\overline{Mn}(py)]$$

$$A_{1920} = 4.0[\overline{Mn}(NCMe)] + 32.4[\overline{Mn}(py)]$$

Since $A_{1934} = 0.213$ and $A_{1920} = 0.231$, $([\overline{Mn}(NCMe)]/[\overline{Mn}(py)])_{eq} = 1.02$. The value $([py]/[NCMe])_{eq}$ is equal to 1.13×10^{-2} and thus $K_{eq} = 1.15 \times 10^{-2}$. Values of K_{eq} evaluated at four other initial concentrations were essentially the same.

Digital Simulation of the Cyclic Voltammograms for Electrocatalytic Ligand Substitution. According to Feldberg's method,[41] the following parameters are required to devise theoretical cyclic voltammograms of the chain mechanism for electrocatalysis given by eq 13, 14, 15, and 16: C_i, the initial concentration of $\overline{Mn}L$; C_j, the initial concentration of added nucleophile L; v, the CV scan rate; E°, the formal potentials of the redox couples $\overline{Mn}L/\overline{Mn}L^+$ and $\overline{Mn}L/\overline{Mn}L^+$; β, the respective transfer coefficients; D, the diffusion coefficients; and the homogeneous rate constants k_1 for ligand exchange in the cation (eq 14) and k_2 for the electron transfer (eq 15). The evaluation of k_1 and k_2 require that all the other electrochemical parameters be determined independently, or at least reasonable estimates made of the error ranges.

Table V. Intrinsic Rate Constants for Various Carbonylmanganese Derivatives $(\eta^5\text{-}C_5H_4Me)Mn(CO)_2L$[a]

L	solvent[a]	k_s,[b] cm s^{-1}
MeCN	MeCN	0.048
MeCN	Me_2CO	[c]
NC_5H_5(py)	Me_2CO	0.038
PEt_3	Me_2CO	0.011
$P(Me)Ph_2$	MeCN	0.030
$P(C_6H_4Me\text{-}p)_3$	MeCN	0.023
PPh_3	MeCN	0.023
PPh_3	Me_2CO	0.032
$P(C_6H_4Cl\text{-}p)_3$	MeCN	0.035
$P(OMe)Ph_2$	MeCN	0.021
$P(OPh)_3$	MeCN	0.015

[a] Solvent contains 0.1 N TEAP at 25 °C. [b] Determined by the procedure in ref 24. [c] Assumed to be 0.048 cm s^{-1} for digital simulation.

The formal potentials E° are well approximated by the CV peak parameters and expressed as[62] $E^\circ \simeq (E_p^{ox} + E_p^{red})/2$ for the carbonylmanganese derivations $\overline{Mn}L$ and $\overline{Mn}L$. The intrinsic rate constants for heterogeneous electron transfer k_s can be dertermined from the scan-rate dependence of $E_p^{ox} - E_p^{red}$, as described previously.[28,77] The values of k_s evaluated in this manner are listed in Table V and lie between 0.01 and 0.05 cm s^{-1}. The transfer coefficients β are close to 0.5 for all the carbonylmanganese derivatives, as qualitatively indicated by the symmetry of the quasi-reversible anodic waves.[24] The diffusion coefficients are known not to be highly structure dependent,[78] and we have thus taken all species to have the same values of D as that of ferrocene (i.e., 2.4×10^{-5} cm^2 s^{-1} at room temperature in MeCN). The assumption that all diffusion coefficients are equal has been employed by others who have studied ECE processes.[38]

In order to determine how the electrochemical parameters affect the theoretical cyclic voltammograms, we have initially chosen an arbitrary set for a system consisting of 0.0017 M $\overline{Mn}(NCMe)$ and 0.0051 M PPh_3 in acetonitrile as $k_1 = 1.3 \times 10^4$ M^{-1} s^{-1}, $k_2 = 5 \times 10^5$ M^{-1} s^{-1}, $k_s[\overline{Mn}(NCMe)] = 0.048$ cm s^{-1}, $k_s[\overline{Mn}(PPh_3)] = 0.023$ cm s^{-1}, $v = 0.4$ V s^{-1}, $\beta[\overline{Mn}(NCMe)] = \beta[\overline{Mn}(PPh_3)] = 0.5$, $D = 2.4 \times 10^{-5}$ cm^2 s^{-1}. The theoretical cyclic voltammogram A in Figure 10 is in fact the same as that presented as the second cyclic voltammogram in Figure 6A. Let us now systematically vary each electrochemical parameter to determine its effect on the cyclic voltammogram.

In Figure 10B, the diffusion coefficient has been increased 2-fold compared to that in Figure 10A, and in Figure 10C it has been decreased by a factor of 2.5. In Figure 10D, only the diffusion coefficient of PPh_3 has been doubled. In each case, little or no change in the theoretical CV is apparent. (Although the anodic current depends on $D^{1/2}$, the observed effect arises from Feldberg's simulation program in which a factor of $D^{-1/2}$ is included in the output.) However, the strong dependence of the cyclic voltammogram on the exchange rate constant $k_1 = 1.3 \times 10^4$ M^{-1} s^{-1} is clearly shown in Figures 10E ($k_1 = 2.0 \times 10^4$ M^{-1} s^{-1}), 10F ($k_1 = 1.0 \times 10^5$ M^{-1} s^{-1}), 10G ($k_1 = 7.0 \times 10^3$ M^{-1} s^{-1}), and 10H ($k_1 = 2 \times 10^2$ M^{-1} s^{-1}). Very large changes in the electron-transfer rate constant k_2 effect only minor changes in the cyclic voltammograms, as shown in Figure 10I ($k_2 = 1.0 \times 10^8$ M^{-1} s^{-1}) and 10J ($k_2 = 7 \times 10^2$ M^{-1} s^{-1}). The magnitudes of the transfer coefficient do not strongly influence the anodic peak current of $\overline{Mn}(NCMe)$, as shown in Figure 10K, in which only $\beta[\overline{Mn}(PPh_3)]$ has been increased from 0.5 to 0.8, and in Figure 10L, in which only $\beta[\overline{Mn}(NCMe)]$ has been increased to 0.8. These simulation experiments thus show that the cyclic voltammogram, particularly the anodic peak current i_p^a, is relatively insensitive to variations in k_2, D, and β. By contrast, minor variations in the exchange rate constant are easily distinguished in Figures 10, E–H, and allow k_1 to be readily optimized

(75) Bayerl, B.; Schmidt, K.; Wahren, M. *Z. Chem.* **1975**, *15*, 277.
(76) See: (a) Adamson, A. W.; Fleishauer, P. D. "Concepts in Inorganic Photochemistry"; Wiley: New York, 1975. (b) Geoffrey, G. L.; Wrighton, M. S. "Organometallic Photochemistry"; Academic Press: New York, 1979.
(77) Klingler, R. J.; Kochi, J. K. *J. Phys. Chem.* **1981**, *85*, 1731.
(78) See: Adams, R. N. "Electrochemistry at Solid Electrodes"; Dekker: New York, 1969, p 216 ff.

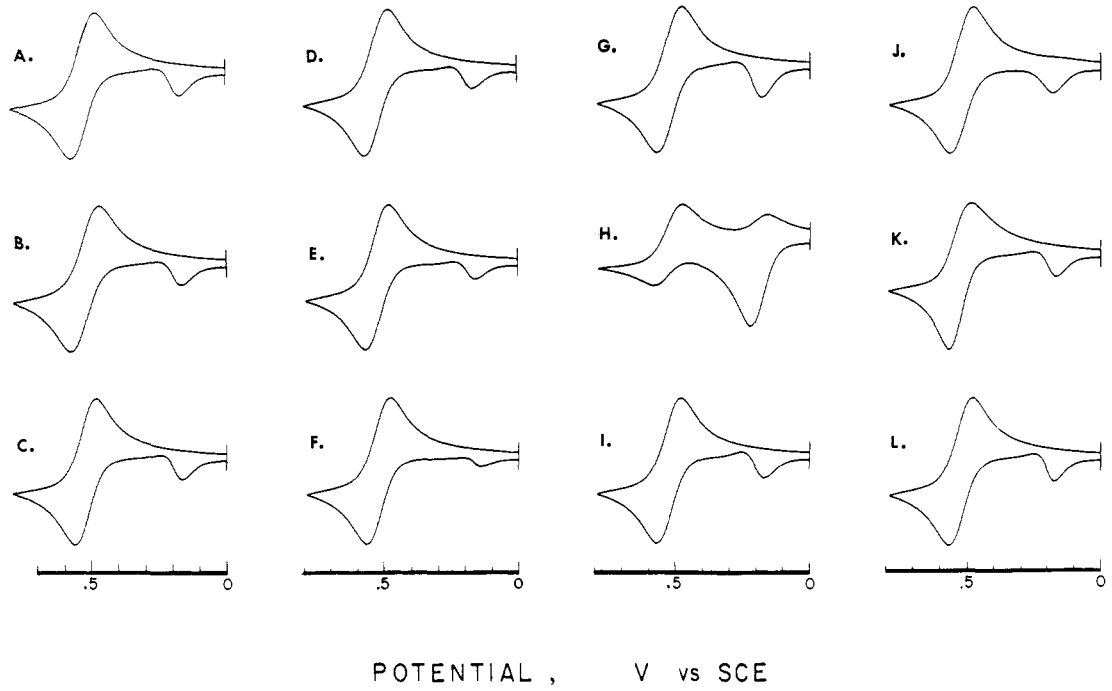

Figure 10. The effect of the electrochemical parameters on the simulated CV for the catalytic ligand substitution by thye ECE process. See text for the variations employed.

with a precision of 15–20%. Coupled with the test of k_1 by variations in the sweep rate and the concentration of $\overline{\text{Mn}}\text{L}$ and ***L*** in Figures 5 and 6, respectively, reliable values of k_1 can be determined for electrocatalytic ligand substitution.

Diffusion coefficients D were determined by the procedure described by Adams,[78] using chronoamperometry and assuming semiinfinite linear diffusion. Current–time profiles were recorded with a PAR Model 4102 signal recorder for later output onto the X–Y recorder. Plots of $it^{1/2}$ vs. t were linear for at least 6–10 s for experiments performed at room temperature, and for longer periods at reduced temperatures. The value of $(it^{1/2})_0$ at zero time was used to calculate the diffusion coefficient from the equation $it^{1/2} = (54.5 \times 10^3)nAD^{1/2}C$.[78] The effective electrode area, A, was evaluated at room temperature by using the known value of D for ferrocene.[78] The same procedure was used to evaluate the diffusion coefficient of ferrocene in acetonitrile containing 0.1 M TEAP at various temperatures as follows: $D \times 10^5$ cm s^2 (°C); 0.76 (−40); 0.86 (−32); 10.7 (−21); 12.7 (−11); 1.70 (0); 2.40 (21). Values of D at intermediate temperatures were determined by interpolation. The lowest temperature was dictated by the freezing point of the solvent and the highest temperature limited by the rate of solvent loss by evaporation.

Competition Experiments for the Direct Determination of the Relative Reactivity of Nucleophiles. A solution containing 0.015 g of (η^5-C_5H_4Me)$Mn(CO)_2$(NCMe) (6.5×10^{-5} mol), 1.07 g of $P(OPh)_3$ (3.4×10^{-3} mol), and 0.050 g of $P(C_6H_4Cl\text{-}p)_3$ (1.37×10^{-4} mol) in 15 mL of a mixture consisting of MeCN and CH_2Cl_2 in a 80:20 volume ratio and containing 0.1 M TEAP was prepared under an inert atmosphere. Electrooxidation at 0.07 V for 20 min in a darkened room resulted in the total conversion of $\overline{\text{Mn}}$(NCMe). The IR analysis of the anolyte (see Table IV) revealed the presence of $\overline{\text{Mn}}[P(C_6H_4Cl\text{-}p)_3]$ and $\overline{\text{Mn}}[P(OPh)_3]$ in a molar ratio of 3.6:1, which corresponds to $k_1[P(OPh)_3]/k_1[P(C_6H_4Cl\text{-}p)_3] = 89$.

A solution containing 0.0271 g of (η^5-C_5H_4Me)$Mn(CO)_2$(NCMe) (1.17×10^{-4} mol), 0.170 g of PPh_3 (6.5×10^{-4} mol), and 0.087 g of $P(C_6H_4Me\text{-}p)_3$ (2.88×10^{-4} mol) was prepared in 15 mL of acetonitrile containing 0.1 M TEAP under an inert atmosphere. Electrooxidation was carried out at 0.07 V for approximately 120 s, since complete conversion was effected. The IR analysis of the anolyte revealed strongly overlapping absorptions in the CO region arising from band broadening. Accordingly, the anolyte was diluted with 150 mL of water, and the resulting precipitate (which contained the mixture of manganese carbonyls and triarylphosphines) was collected by filtration. Dissolution in n-heptane afforded an IR spectrum that was analyzed as a mixture of $\overline{\text{Mn}}(PPh_3)$ and $\overline{\text{Mn}}(C_6H_4Me\text{-}p)_3$ in a 1.1:1.0 ratio. The latter corresponds to a ratio of rate constants $k_1[\overline{\text{Mn}}(PPh_3)]/k_1[\overline{\text{Mn}}(P(C_6H_4Me\text{-}p)_3] = 0.49$. However, owing to difficulties in the IR analysis of similar phosphine derivatives, the uncertainty is estimated to be 50%.

It was necessary to test the importance of ligand exchange in the products $\overline{\text{Mn}}\text{L}$ and $\overline{\text{Mn}}\boldsymbol{L}$ in the presence of ***L*** and L, respectively, as a complicating factor in the competition experiments in the following manner. A mixture of 21 mg of $\overline{\text{Mn}}[P(C_6H_4Cl\text{-}p)_3]$ (5.8×10^{-5} mol) and 590 mg of $P(OPh)_3$ (1.9×10^{-3} mol) was dissolved in 10 mL of acetonitrile containing 0.1 M TEAP. The solution was electrooxidized at a Pt-gauze electrode for 20 min at 200 μA, which corresponded overall to 0.040 faraday of charge per mol of manganese carbonyl. The IR spectrum of the resulting anolyte revealed the presence of a 60:40 mixture of $\overline{\text{Mn}}[P(C_6H_4Cl\text{-}p)_3]$ and $\overline{\text{Mn}}[P(OPh)_3]$, respectively. Although phosphine–phosphite exchange occurred under these rather forcing conditions, it can be reasonably assumed that it would occur only after the reactant $\overline{\text{Mn}}\text{L}$ is consumed. Accordingly, we choose a potential controlled oxidation for these competition studies. Thus the potential was set at the foot of the anodic wave of $\overline{\text{Mn}}\text{L}$ such that the initial current was only 100 μA. Under these conditions, the electrode served only as a reducing agent for $\overline{\text{Mn}}\text{L}^+$ and $\overline{\text{Mn}}\boldsymbol{L}^+$. The completion of the exchange was signaled by an abrupt drop in the anodic current to 0.0 μA.

Acknowledgment. We thank Paul Zizelman for assistance in the preparation of several manganese complexes and the National Science Foundation for financial support and funds to purchase the computer.

Supplementary Material Available: Listing of the Fortran program for the digital simulation of the cyclic voltammograms according to the kinetics in Scheme III (5 pages). Ordering information is given on any current masthead page.